Available online at http://scik.org

Commun. Math. Biol. Neurosci. 2022, 2022:14

https://doi.org/10.28919/cmbn/7056

ISSN: 2052-2541

CHAOS IN THE THREE-SPECIES SOKOL-HOWELL FOOD CHAIN SYSTEM WITH FEAR

FIRAS HUSSEAN MAGHOOL, RAID KAMEL NAJI*

Department of Mathematics, College of Science, University of Baghdad, Baghdad, Iraq

Abstract: In this paper, the influence of predation fear on the dynamics of the three species food chain system is formulated mathematically and investigated. It is assumed that the food is transferred from the lower level to the upper level according to the Sokol-Howell type of functional response due to the anti-predator property of each prey in the system. The boundedness and persistence conditions are established for the proposed food chain system. The local and global stability analysis is investigated. The occurrence conditions of local bifurcation including the Hopf bifurcation near the equilibrium points are obtained. In the end, numerical simulation is performed to validate the theoretical results and present the dynamical behavior of the system. Different mathematical tools such as strange attractor, bifurcation diagram, and Lyapunov exponents are used to detect chaos in the proposed system. It is observed that the model is capable of exhibiting complex dynamics including chaos. It is also pointed out that a suitable predation fear can control the chaotic dynamics and make the system stable.

Keywords: food chain; chaos; stability; bifurcation diagram; Lyapunov exponents.

2010 AMS Subject Classification: 92D40, 34C23, 34C28.

*Corresponding author

E-mail address: rknaji@gmail.com

Received December 03, 2021

1. INTRODUCTION

In ecosystems, prey-predator interactions are critical, and understanding the mechanisms that drive them is a difficult issue in ecology and evolutionary biology. In prey-predator interactions, predation has long been regarded to be the most important factor. A predator eats prey by hunting and killing it in the wild. However, increasing evidence suggests that many animals can predict the likelihood of predation and adjust their behavior accordingly. When prey becomes aware of the possibility of predation, it may engage in anti-predator behaviors like modifying its habits or appearance, as well as shifting its foraging and reproductive times.

Anti-predator behavior in prey is common, and the fear effect can be large, meaning that fear has a big impact on population dynamics. Despite the fact that predators do not kill prey directly, the fear of predators on prey has an impact on predator and prey population dynamics. In fact, there's evidence that the indirect influence can be just as significant as the direct effect. As a result, when researching prey-predator interactions, taking into account solely the direct killing effect is insufficient. Hua et al [1] proposed a two-dimensional prey-predator model that incorporates the cost of fear into prey growth. Several other prey-predator systems incorporating the fear effect have been developed and examined as a result of this research, see [2-12].

As the prey becomes aware of the threat of predation, it may exhibit anti-predator behaviors such as adjusting its habits, foraging times, and reproduction. These responses will have an impact on the prey's population density. To avoid being killed immediately, the prey may choose to stay in a safer area distant from the high-risk sector when foraging. In terms of foraging time, the prey species may choose to restrict its foraging activity at some risk, forcing it to adopt a hungry survival mechanism and, as a result, lowering its growth rate.

On the other hand, prey anti-predator behavior is common, and the fear effect can be significant, implying that fear has a significant impact on population dynamics. Wang et al [7-8] created a two-dimensional prey-predator model adding the cost of fear into prey growth with this motivation. Their findings suggest that the anti-predator reaction is critical in maintaining the prey-predator balance. They also discovered that in the model incorporating the cost of fear, the Hopf bifurcation

can occur and can be both supercritical and subcritical, which differs from previous conventional prey-predator models. Pal et al. [11] looked at the fear effect in a prey-predator model in which the prey-predator interaction follows the Beddington–DeAngelis functional response. They discovered that as the cost of fear rises, the system becomes unstable and provides periodic solutions via supercritical Hopf bifurcation. The system, however, experiences another Hopf bifurcation and becomes stable as the level of fear increases, similar findings were found in [10-11]. Recently, Sarkar and Khajanchi [12] designed and examined a prey-predator system with Holling type-II functional response that introduced the cost of fear into prey reproduction. They showed that powerful anti-predator reactions can stabilize prey-predator interactions by ignoring the occurrence of the periodic activity.

Following these studies, other scientists used the Holling type II function response to represent the feeding process in a tri-trophic food chain and food web models. Panday et al [13] suggested and explored the influence of fear in a tri-trophic food chain model, in which the growth rate of the middle predator is reduced owing to the cost of top predator fear, and the growth rate of prey is repressed due to the cost of middle predator fear. Fear, they discovered, may settle the system from chaos to stable focus by half the period, similar findings were found in [14]. Later, Ibrahim and Naji [15] investigated the influence of fear in the Beddington–DeAngelis food chain model with three species. They discovered that fear has a stabilizing influence on the system up to a threshold degree; otherwise, it acts as an extinction factor in the system. Mukherjee provided a mathematical model that simulates two competing prey and one predator system with the cost of fear that impacts both the prey population's reproduction rate and the predator's predation rate in [16]. He observed that although a high level of fear can make coexistence impossible, a rise in intraspecific competition within the predator population can allow predator and competitive prey to coexist. In [17], Abd and Naji devised and analyzed a food chain model that included fear at the first and second levels. Alternative food sources for the top predator are also taken into account. They obtained that the system has many dynamics, including chaos, which can be decreased by increasing the fear rate. Maghool and Naji recently suggested and investigated the dynamics of a

tri-trophic Leslie-Gower food-web system under the influence of fear [18]. They discovered that the fear factor acts as a system stabilizer up to a certain point, after which it causes the predator to become extinct.

In contrast to prior researches, this publication considers the impact of fear from predator predation in the upper level of the food chain throughout the levels of the food chain in which the prey species has an anti-predator capability such as group defense. The following is the outline of the paper: Section 2 describes the model and its dimensionless form. Section 3 defines the equilibrium points and describes the conditions that must be met for them to be stable locally. The model's persistence is discussed in Section 4, and the research of global behavior is discussed in Section 5. Section 6 investigates the feasibility of local bifurcation, while section 7 determines the criteria for Hopf bifurcation to occur. Moreover, section 8 applies numerical simulation to test our theoretical findings and discovers chaos by producing bifurcation diagrams and Lyapunov exponent bifurcation diagrams. Finally, the conclusion and discussion of this work are given in section 9.

2. THE MODEL FORMULATION

In the present section, the real-world three-species food chain system is formulated mathematically. It is assumed that fear affects negatively the growth rates of the prey and middle predator. Furthermore, the middle predator's fear of predation from the upper predator reduces the middle predator's foraging too. Accordingly, the predation rate of the middle predator and the growth rate of the prey at the first level, and that of the middle predator at the second level are multiplied by a decreasing function of upper predator population density. On the other hand, it is assumed that the preys have an anti-predator technique capability against predation by the predator at the upper level. Consequently, the dynamics of the above described food chain system can be represented by the following set of first order nonlinear differential equations. The terms $\frac{1}{1+n_1Y}$, and $\frac{1}{1+n_2Z}$ represent the reduction in the growth rate of the prey, and the reduction in the growth rate and foraging of the middle predator due to the fear. While the Sokol-Howell type of functional

responses are used to describe the predation process due to the existence of the anti-predator technique. Therefore, the above described real world food-chain system can be represented mathematically using the following system of differential equations.

$$\begin{aligned}\frac{dX}{dT} &= \frac{rX}{(1+n_1Y)} - bX^2 - \frac{a_0XY}{1+m_0X^2}\left(\frac{1}{1+n_2Z}\right),\\ \frac{dY}{dT} &= \frac{a_1XY}{1+m_0X^2}\left(\frac{1}{1+n_2Z}\right) - \frac{a_2YZ}{1+m_1Y^2} - d_0Y,\\ \frac{dZ}{dT} &= \frac{a_3YZ}{1+m_1Y^2} - d_1Z,\end{aligned} \tag{1}$$

with $X(0) \geq 0, Y(0) \geq 0, and\ Z(0) \geq 0$, where $X(T)$ represents the prey density at the time T, $Y(T)$ is the middle predator density at the time T, while $Z(T)$ is the top predator density at time T. The parameters in the system (1) are assumed to be positive and are detailed in the Table (1) below.

Table 1: The description of the model (1) parameters

Parameter	Description
r	The intrinsic growth rate of the prey population.
b	Intraspecific competition of the prey.
$a_0,\ a_2$	Maximum attack rates of the middle predator and top predator respectively.
$a_1,\ a_3$	Conversion rates to the middle predator and top predator respectively.
n_1, n_2	Fear levels from the middle predator and top predator respectively.
$m_0,\ m_1$	Preference rates for the middle predator and top predator respectively.
d_0, d_1	Natural mortality rates of middle predator and top predator respectively.

Clearly, system (1) has eleven parameters in all. Therefore for easier mathematical analysis, the number of parameters is reduced using the following transformations.

$$x = \frac{bX}{r}, y = \frac{a_0Y}{r}, z = \frac{a_1Z}{r}, t = rT,\ u_1 = \frac{n_1r}{a_0},\quad u_2 = \frac{m_0r^2}{b^2}, u_3 = \frac{n_2r}{a_1},$$

$$u_4 = \frac{a_1}{b},\ u_5 = \frac{a_2}{a_1}, u_6 = \frac{m_1r^2}{{a_0}^2}, u_7 = \frac{d_0}{r},\ u_8 = \frac{a_3}{a_0}, u_9 = \frac{d_1}{r}.$$

Therefore, the non-dimensional system that corresponds to the system (1) is given by:

$$\begin{aligned}\frac{dx}{dt} &= x\left[\frac{1}{1+u_1y} - x - \frac{y}{1+u_2x^2}\left(\frac{1}{1+u_3z}\right)\right] = xf_1(x,y,z),\\ \frac{dy}{dt} &= y\left[\frac{u_4x}{1+u_2x^2}\left(\frac{1}{1+u_3z}\right) - \frac{u_5z}{1+u_6y^2} - u_7\right] = yf_2(x,y,z),\\ \frac{dz}{dt} &= z\left[\frac{u_8y}{1+u_6y^2} - u_9\right] = zf_3(x,y,z).\end{aligned} \tag{2}$$

Here, the interaction functions are define on $\mathbb{R}_+{}^3 = \{(x,y,z): x(t) \geq 0, y(t) \geq 0, z(t) \geq 0\}$. Moreover, since the interaction functions in the right-hand side of the system (2) are continuous and have a continuous partial derivatives, hence they are Lipschitzian functions. Thus, the solution of the system (2) exists and is unique.

Theorem 1: All the solutions of the system (2), which initiate in $\mathbb{R}_+{}^3$ are uniformly bounded.

Proof. Let $(x(t), y(t), z(t))$ be the solution of system (2), then from the first equation, it is obtained that $\frac{dx}{dt} \leq x - x^2$, then as $t \to \infty$ the following is obtained $x \leq 1$.

Define the function $M(t) = u_4x(t) + y(t) + \frac{u_5}{u_8}z(t)$.

Differentiating the function $M(t)$, yields:

$$\frac{dM}{dt} = u_4\frac{dx}{dt} + \frac{dy}{dt} + \frac{u_5}{u_8}\frac{dz}{dt} = \frac{u_4x}{1+u_1y} - u_4x^2 - u_7 - \frac{u_5u_9}{u_8}z.$$

Then

$$\frac{dM}{dt} \leq 2u_4x - \left[u_4x - u_7y - \frac{u_5u_9}{u_8}z\right] \leq 2u_4 - \delta M,$$

where $\delta = \min\{1, u_7, u_9\}$. Consequently, as $t \to \infty$, it is obtain that

$$M(t) \leq \frac{2u_4}{\delta}.$$

Hence the solutions of the system (2) with non-negative initial point are uniformly bounded in the region $\aleph = \left\{(x,y,z) \in \mathbb{R}_+{}^3, 0 < u_4x(t) + y(t) + \frac{u_5}{u_8}z(t) \leq \frac{2u_4}{\delta}\right\}$.

3. EQUILIBRIUM POINTS AND LOCAL STABILITY ANALYSIS

The system (2) has at most four non-negative equilibrium points, the form of points with their existence conditions are stated below.

1. The trivial equilibrium point (TEP) that is denoted by $e_0 = (0,0,0)$ always exists.
2. The axial equilibrium point (AEP) that is denoted by $e_1 = (1,0,0)$ always exists.

3. The top predator free equilibrium point TPFEP, which is denoted by $e_2 = (\bar{x}, \bar{y}, 0)$, of the system (2) can be obtained by solving the following system of equations.

$$u_1 y^2 + (1 + u_1 x + u_1 u_2 x^3) y - (1 - x)(1 + u_2 x^2) = 0$$
$$u_2 u_7 x^2 - u_4 x + u_7 = 0$$

Straightforward computation shows that the above system has a unique positive solution in the interior of xy −plane that is given by Eq. (3) provided that the conditions given by Eq. (4) hold together.

$$\bar{x} = \frac{u_4 - \sqrt{{u_4}^2 - 4u_2 {u_7}^2}}{2u_2 u_7},\ \bar{y} = \frac{-B + \sqrt{B^2 + 4AC}}{2A}, \tag{3}$$

where $A = u_1,\ B = u_1 \bar{x} + u_1 u_2 \bar{x}^3 + 1$, and $C = -(\bar{x} - 1)(1 + u_2 \bar{x}^2)$.

$$4{u_7}^2 u_2 < {u_4}^2,$$
$$\bar{x} < 1. \tag{4}$$

4. The coexistence equilibrium point (CEP), that is denoted by $e_3 = (x^*, y^*, z^*)$, exists uniquely in the interior of positive octant if and only if there is a unique solution to the following set of algebraic equations.

$$\frac{1}{1+u_1 y} - x - \frac{y}{1+u_2 x^2}\left(\frac{1}{1+u_3 z}\right) = 0,$$
$$\frac{u_4 x}{1+u_2 x^2}\left(\frac{1}{1+u_3 z}\right) - \frac{u_5 z}{1+u_6 y^2} - u_7 = 0, \tag{5}$$
$$\frac{u_8 y}{1+u_6 y^2} - u_9 = 0.$$

Although the third equation has two positive solutions given by the equation (6), the algebraic system (7) that results from the first two equations of (5) after substituting the value of $y_i^*; i = 1,2$ may or may not have a unique intersection point depending on the value of the parameters.

$$y_{1,2}^* = \frac{u_8 \mp \sqrt{{u_8}^2 - 4u_6 {u_9}^2}}{2u_6 u_9}. \tag{6}$$

$$H_1(x, z) = \frac{1}{1+u_1 y_i^*} - x - \frac{y_i^*}{(1+u_2 x^2)(1+u_3 z)} = 0,$$
$$H_2(x, z) = \frac{u_4 x}{(1+u_2 x^2)(1+u_3 z)} - \frac{u_5 z}{1+u_6 {y_i^*}^2} - u_7 = 0. \tag{7}$$

For instance, for the parameter values:

$$u_1 = 0.25, u_2 = 2, u_3 = 0.25, u_4 = 1, u_5 = 1, u_6 = 2, u_7 = 0.1, u_8 = 1, u_9 = 0.1. \tag{8}$$

From equation (6), there are two positive values of y, given by $y_1^* = 0.102084$ and $y_2^* =$

4.89792. However system (7) has a unique solution given by $(x^*, z^*) = (0.94, 0.22)$ at y_1^*, while it has no solution at y_2^*, see Figure (1a) and (1b) respectively. Therefore for the set of data (8), the system (2) has a unique CEP given by $e_3 = (0{,}94{,}0.1{,}0.22)$.

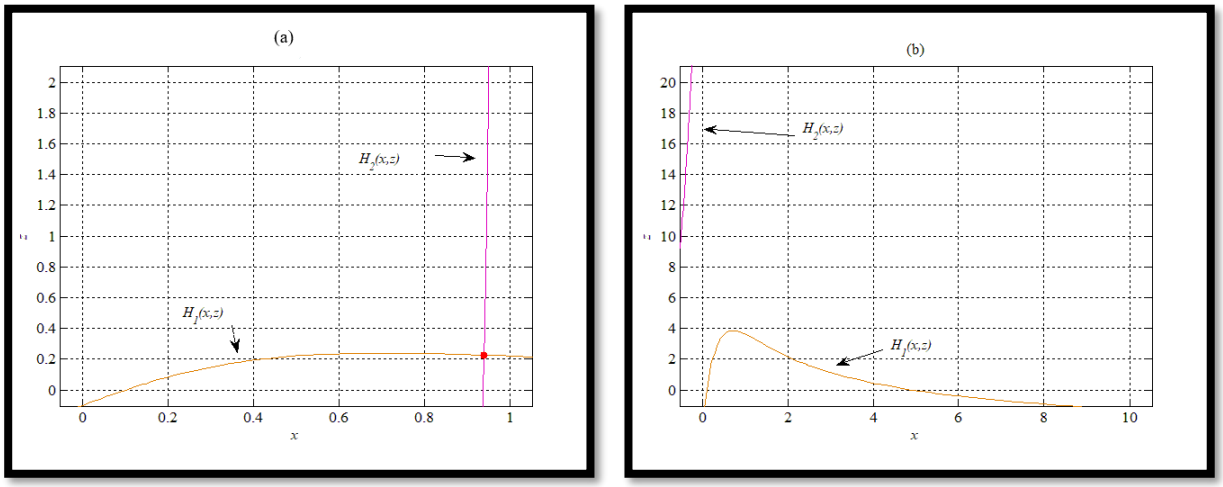

Figure 1: Existence of CEP. (a) The unique solution of system (7) when $y_1^* = 0.102084$. (b) There is no solution when $y_2^* = 4.89792$

In the following the local stability analysis of the system (2) near the above equilibrium points is investigated using the linearization technique.

The Jacobin matrix of system (2) at the point (*x, y, z*) can be written as:

$$J = \begin{pmatrix} x\frac{\partial f_1}{\partial x} + f_1 & x\frac{\partial f_1}{\partial y} & x\frac{\partial f_1}{\partial z} \\ y\frac{\partial f_2}{\partial x} & y\frac{\partial f_2}{\partial y} + f_2 & y\frac{\partial f_2}{\partial z} \\ z\frac{\partial f_3}{\partial x} & z\frac{\partial f_3}{\partial y} & z\frac{\partial f_3}{\partial z} + f_3 \end{pmatrix} = (a_{ij})_{3\times 3}, \tag{9}$$

where $a_{11} = -x + \frac{2u_2x^2y}{\eta_1^2\eta_3} + \left(\frac{1}{\eta_2} - x - \frac{y}{\eta_1\eta_3}\right)$, $a_{12} = \frac{-u_1x}{\eta_2^2} - \frac{x}{\eta_1\eta_3}$, $a_{13} = \frac{u_3xy}{\eta_1\eta_3^2}$, $a_{21} = \frac{u_4y(1-u_2x^2)}{\eta_1^2\eta_3}$, $a_{22} = \frac{2u_5u_6y^2z}{\eta_4^2} + \left(\frac{u_4x}{\eta_1\eta_3} - \frac{u_5z}{\eta_4} - u_7\right)$, $a_{23} = \frac{-u_3u_4xy}{\eta_1\eta_3^2} - \frac{u_5y}{\eta_4}$, $a_{31} = 0$, $a_{32} = \frac{u_8z(1-u_6y^2)}{\eta_4^2}$, $a_{33} = \frac{u_8y}{\eta_4} - u_9$, with $\eta_1 = 1 + u_2x^2$, $\eta_2 = 1 + u_1y$, $\eta_3 = 1 + u_3z$, and $\eta_4 = 1 + u_6y^2$.

Therefore, the following can be obtain:

The Jacobian matrix at TEP has the eigenvalues $\lambda_{01} = 1,\ \lambda_{02} = -u_7,\ \lambda_{03} = -u_9$, and hence e_0 is a saddle point.

The Jacobian matrix at AEP has the eigenvalues $\lambda_{11} = -1,\ \lambda_{12} = \frac{u_4}{1+u_2} - u_7$, and $\lambda_{13} = -u_9$, hence e_1 is a locally asymptotically stable provided that

$$\frac{u_4}{1+u_2} < u_7. \tag{10}$$

The Jacobian matrix at TPFEP is reduced to:

$$J_{e_2} = \left(b_{ij}\right)_{3x3}, \tag{11a}$$

where $b_{11} = -\bar{x} + \frac{2u_2\bar{x}^2\bar{y}}{\bar{\eta}_1^2},\ b_{12} = \frac{-u_1\bar{x}}{\bar{\eta}_2^2} - \frac{\bar{x}}{\bar{\eta}_1},\ b_{13} = \frac{u_3\bar{x}\,\bar{y}}{\bar{\eta}_1},\ b_{21} = \frac{u_4\bar{y}(1-u_2\bar{x}^2)}{\bar{\eta}_1^2},\ b_{22} = 0,\ b_{23} = \frac{-u_3u_4\bar{x}\bar{y}}{\bar{\eta}_1} - \frac{u_5\bar{y}}{\bar{\eta}_4},\ b_{31} = 0,\ b_{32} = 0,\ b_{33} = \frac{u_3\bar{y}}{\bar{\eta}_4} - u_9$, with $\bar{\eta}_1 = 1 + u_2\bar{x}^2,\ \bar{\eta}_2 = 1 + u_1\bar{y},\ \bar{\eta}_4 = 1 + u_6\bar{y}^2$.

Therefore, the characteristic equation of J_{e_2} can be written as:

$$[\lambda^2 - b_{11}\lambda - b_{12}b_{21}](b_{33} - \lambda) = 0. \tag{11b}$$

Clearly, the eigenvalues of the Eq. (11b) can be written as:

$$\lambda_{21} = \frac{b_{11}+\sqrt{(b_{11})^2+4b_{12}b_{21}}}{2},\ \lambda_{22} = \frac{b_{11}-\sqrt{(b_{11})^2+4b_{12}b_{21}}}{2},\ \lambda_{23} = \frac{u_3\bar{y}}{\bar{\eta}_4} - u_9. \tag{12}$$

It is easy to verify that, all the eigenvalues of J_{e_2} are negative, and hence e_2 is locally asymptotically stable, provided that the following conditions hold:

$$\frac{2u_2\bar{x}\bar{y}}{\bar{\eta}_1{}^2} < 1, \tag{13a}$$

$$\bar{x}^2 < \frac{1}{u_2}, \tag{13b}$$

$$\frac{u_3\bar{y}}{\bar{\eta}_4} < u_9. \tag{13c}$$

The Jacobian matrix of the system (2) at the CEP can be written as:

$$J_{e_3} = \left(c_{ij}\right)_{3x3}, \tag{14}$$

where:

$$c_{11} = -x^* + \frac{2u_2x^{*2}y^*}{\eta_{1*}^2\eta_{3*}},\ c_{12} = -\frac{u_1x^*}{\eta_{2*}^2} - \frac{x^*}{\eta_{1*}\eta_{3*}},\ c_{13} = \frac{u_3x^*y^*}{\eta_{1*}\eta_{3*}^2},$$

$$c_{21} = \frac{u_4 y^*\left(1-u_2 x^{*2}\right)}{\eta_{1*}^2 \eta_{3*}},\ c_{22} = \frac{2u_5 u_6 y^{*2} z^*}{\eta_{4*}^2},\ c_{23} = -\frac{u_3 u_4 x^* y^*}{\eta_{1*}\eta_{3*}^2} - \frac{u_5 y^*}{\eta_{4*}},$$

$$c_{31} = 0,\ c_{32} = \frac{u_8 z^*(1-u_6 y^{*2})}{\eta_{4*}^2},\ c_{33} = 0.$$

with $\eta_{1*} = 1 + u_2 x^{*2},\ \eta_{2*} = 1 + u_1 y^*,\ \eta_{3*} = 1 + u_3 z^*,\ \eta_{4*} = 1 + u_6 y^{*2}$. Consequently, the characteristic equation of J_{e_3} can be written as:

$$\lambda^3 + A_1\lambda^2 + A_2\lambda + A_3 = 0, \tag{15}$$

where $A_1 = -(c_{11} + c_{22})$, $A_2 = c_{11}c_{22} - c_{12}c_{21} - c_{23}c_{32}$, and $A_3 = c_{32}[c_{11}c_{23} - c_{13}\,c_{21}]$, with $\Delta = A_1A_2 - A_3 = -(c_{11} + c_{22})(c_{11}c_{22} - c_{12}c_{21}) + c_{32}(c_{22}c_{23} + c_{13}c_{21})$.

Now, according to Routh-Hurwitz criterion, all the eigenvalues of the characteristic equation (15) have negative real parts and then the CEP becomes locally asymptotically stable if and only if $A_1 > 0,\ A_3 > 0$, and $\Delta > 0$. Accordingly, the following theorem can be proved easily.

Theorem (2): The CEP is locally asymptotically stable if the following sufficient conditions hold.

$$x^{*2} < \frac{1}{u_2}, \tag{16a}$$

$$y^{*2} < \frac{1}{u_6}, \tag{16b}$$

$$\frac{2u_2 x^{*2} y^* \eta_{4*}^2 + 2u_5 u_6 y^{*2} z^* \eta_{1*}^2 \eta_{3*}}{\eta_{1*}^2 \eta_{3*} \eta_{4*}^2} < x^*, \tag{16c}$$

$$u_3 u_4 y^* \eta_{4*}\left(1 - u_2 x^{*2}\right) < (\eta_{1*}^2 \eta_{3*} - 2u_2 x^* y^*)(u_3 u_4 x^* \eta_{4*} + u_5 \eta_{1*} \eta_{3*}^2), \tag{16d}$$

$$2u_5 u_6 y^* z^* (\eta_{1*}^2 \eta_{3*} - 2u_2 x^* y^*)\eta_{1*}\eta_{2*}^2 \eta_{3*} < u_4(u_1 \eta_{1*}\eta_{3*} + \eta_{2*}^2)\left(1 - u_2 x^{*2}\right)\eta_{4*}^2, \tag{16e}$$

$$u_3 u_4 x^*\left(1 - u_2 x^{*2}\right)\eta_{1*}^3 > 2u_5 u_6 y^* z^* \eta_{1*}^2 \eta_{3*}(u_3 u_4 x^* \eta_{4*} + u_5 \eta_{1*} \eta_{3*}^2). \tag{16f}$$

4. PERSISTENCE

The persistence of the system (2) is studied, it is well known that the system is said to persist if and only if each species persist, mathematically this means that the system (2) persists if the solution of the system with the positive initial condition does not have omega limit set on the boundary of its domain.

The system (2) has a subsystem lying in the positive quadrant of xy −plane, which can be written

as follow:

$$\begin{aligned}\frac{dx}{dt} &= x\left[\frac{1}{1+u_1 y} - x - \frac{y}{1+u_2 x^2}\right] = \mu_1\,(x,y),\\ \frac{dy}{dt} &= y\left[\frac{u_4 x}{1+u_2 x^2} - u_7\right] = \mu_2\,(x,y),\end{aligned} \tag{17}$$

It is easy to verify that, this subsystem has a positive equilibrium point coincide with the TPFEP of the system (2) in the interior of the positive quadrant of the xy −plane. Now, to discover the possibility of the existence of periodic dynamics around the interior positive point of the subsystem (17), the Dulac function approach is used.

Define the function $\varpi\,(x,y) = \frac{1}{xy}$. Clearly this function is continuously differentiable function in the interior of the positive quadrant of the xy −plane and $\varpi\,(x,y) > 0$, for all $(x,y) \in \mathbb{R}^2_+$. Furthermore, direct computation gives that

$$\Delta(x,y) = \frac{\partial}{\partial x}(\varpi \cdot \mu_1) + \frac{\partial}{\partial y}(\varpi \cdot \mu_2) = -\frac{1}{y} + \frac{2u_2 x}{(1+u_2 x^2)^2}.$$

Therefore, $\Delta(x,y)$ does not change sign and not identically to zero under the following condition:

$$\frac{2u_2 xy}{(1+u_2 x^2)^2} < 1. \tag{18}$$

Note that, condition (18) is coincide with condition (13a) at the TPFEP, which means the subsystem (17) is a globally asymptotically stable in the interior of the positive quadrant of the xy −plane whenever the subsystem has a locally asymptotically stable in the interior of $\mathbb{R}^2_+$. Hence, according to the Dulac approach, there is no periodic dynamics in the interior of positive quadrant of xy −plane for the subsystem.

Theorem (3): Assume that there are no periodic dynamics in the boundary planes, then the system (2) is uniformly persistent provided that the following conditions hold

$$u_7 < \frac{u_4}{1+u_2}, \tag{19a}$$

$$u_9 < \frac{u_3 \bar{y}}{1+u_6 \bar{y}^2}, \tag{19b}$$

Proof. Define $\phi(x,y,z) = x^{q_1} y^{q_2} z^{q_3}$, where p_1, p_2, p_3 are positive constants, and $\phi(x,y,z) > 0$ for all $(x,y,z) \in Int\ {\mathbb{R}_+}^3$ with $\phi(x,y,z) = 0$ if any one of x, y, or z

approaches zero. Therefore, direct computation gives:

$$\Omega(x,y,z) = \frac{\phi'(x,y,z)}{\phi(x,y,z)} = q_1 f_1 + q_2 f_2 + q_3 f_3,$$

where the functions $f_i; i = 1,2,3$, are given in the system (2). Now, according to the average Lyapunov method, the proof is as follows provided that $\Omega(x,y,z) > 0$ for all boundary equilibrium points. Therefore,

$$\Omega(x,y,z) = q_1\left[\frac{1}{1+u_1 y} - x - \frac{y}{1+u_2 x^2}\left(\frac{1}{1+u_3 z}\right)\right]$$
$$+q_2\left[\frac{u_4 x}{1+u_2 x^2}\left(\frac{1}{1+u_3 z}\right) - \frac{u_5 z}{1+u_6 x^2} - u_7\right] + q_3\left[\frac{u_8 y}{1+u_6 y^2} - u_9\right].$$

We have that

$$\Omega(e_0) = q_1 + q_2[-u_7] + q_3[-u_9].$$

Obviously, by choosing the arbitrary positive value of q_1 sufficiently large with respect to q_2, q_3, it is obtained that $\Omega(e_0) > 0$.

$$\Omega(e_1) = q_2\left[\frac{u_4}{1+u_2} - u_7\right] + q_3[-u_9].$$

Note that, the condition (19a) guarantees that the coefficient of q_2 is positive, then by suitable chose of the parameters q_2 and q_3, so that q_2 is sufficiently large with respect to q_3, it is obtain that $\Omega(e_1) > 0$. Now, regarding to TPFEP, we have:

$$\Omega(e_2) = q_3\left[\frac{u_8 \bar{y}}{1+u_6 \bar{y}^2} - u_9\right].$$

Clearly, the condition (19b) guarantees that $\Omega(e_2) > 0$.

Hence the system (2) is uniformly persistent, and the proof is complete.

5. GLOBAL STABILITY ANALYSIS

In this section, the global stability of the locally asymptotically stable equilibrium points of system (2) is investigated using suitable Lyapnuov functions as shown in the following theorems.

Theorem (4): Assume that the AEP is locally asymptotically stable and the following conditions hold then it is a globally asymptotically stable.

$$u_4(1 + u_1) < u_7, \tag{20}$$

Proof. Define the real valued function $N_1(x,y,z) = u_4(x-1-\ln x)+y+\frac{u_5}{u_8}z$.

Clearly the function $N_1(x,y,z)$ is a positive definite function that is $N_1(1,0,0)=0$, while $N_1(x,y,z)>0$, for all values in the region $\{(x,y,z)\in {\mathbb{R}_+}^3 : x>0, y\geq 0, z\geq 0;\ (x,y,z)\neq (1,0,0)\}$. Then using some algebraic manipulation give that:

$$\frac{dN_1}{dt} = -u_4(x-1)^2+\frac{u_4(x-1)}{1+u_1y}-\frac{u_4(x-1)y}{(1+u_2x^2)(1+u_3z)} - u_4(x-1)+\frac{u_4xy}{(1+u_2x^2)(1+u_3z)}-\frac{u_5yz}{1+u_6y^2} - u_7y+\frac{u_5yz}{1+u_6y^2}-\frac{u_5\,u_9}{u_8}z$$

Consequently, by using additional computation the following is obtained:

$$\frac{dN_1}{dt}\leq -u_4(x-1)^2-[\,u_7-u_4(1+u_1)\,]y-\frac{u_5\,u_9}{u_8}z.$$

Now by using the condition (20), it is observed that $\frac{dN_1}{dt}<0$, which means it is a negative definite. Therefore, the AEP is globally asymptotically stable. ■

Theorem (5): Assume that the TPFEP is locally asymptotically stable, then all the trajectories of the system (2) starting from points belong to the sub-region of ${\mathbb{R}_+}^3$, which satisfies the following sufficient conditions, approach asymptotically to TPFEP.

$$\frac{u_2\bar{y}(1+\bar{x})}{\bar{\eta}_1}<1, \tag{21a}$$

$$\left[\frac{u_1}{\eta_2\bar{\eta}_2}+\frac{1}{\eta_1\eta_3}-\frac{1}{\eta_1\bar{\eta}_1\eta_3}+\frac{u_2x\bar{x}}{\eta_1\bar{\eta}_1\eta_3}\right]^2<4\left[1-\frac{u_2\bar{y}(1+\bar{x})}{\bar{\eta}_1}\right], \tag{21b}$$

$$0<\frac{u_4(y-\bar{y})^2}{\left[\frac{u_5u_9}{u_8}-\frac{u_3\,u_4\bar{y}}{\bar{\eta}_1}-u_5\bar{y}\right]}<z. \tag{21c}$$

where the symbols η_i and $\bar{\eta}_i$ for $i=1,2,3,4$ are given in Eqs. (9) and (11a) respectively.

Proof. Define the real valued function

$$N_2(x,y,z) = u_4\left(x-\bar{x}-\bar{x}\ln\left(\frac{x}{\bar{x}}\right)\right)+\left(y-\bar{y}-\bar{y}\ln\left(\frac{y}{\bar{y}}\right)\right)+\frac{u_5}{u_8}z.$$

Clearly the function $N_2(x,y,z)$ is a positive definite function that is $N_2(\bar{x},\bar{y},0)=0$, while $N_2(x,y,z)>0$, for all values in the region $\{(x,y,z)\in {\mathbb{R}_+}^3 : x>0, y>0, z\geq 0;\ (x,y,z)\neq$

$(\bar{x}, \bar{y}, 0)\}$. Then for any initial point (x, y, z) that belongs to the sub-region satisfying the above condition, it is obtained that:

$$\frac{dN_2}{dt} = u_4(x-\bar{x})\left[-(x-\bar{x}) - \frac{u_1(y-\bar{y})}{\eta_2\bar{\eta}_2} - \frac{(y-\bar{y})}{\eta_1\eta_3} + \frac{u_2\bar{y}\ (x^2-\bar{x}^2)}{\eta_1\bar{\eta}_1\eta_3} + \frac{u_3\bar{y}z}{\bar{\eta}_1\eta_3}\right] + (y-\bar{y})\left[\frac{u_4(x-\bar{x})}{\eta_1\bar{\eta}_1\eta_3} - \frac{u_2u_4x\bar{x}(x-\bar{x})}{\eta_1\bar{\eta}_1\eta_3} - \frac{u_3u_4\ z\bar{x}}{\bar{\eta}_1\eta_3} - \frac{u_5z}{\eta_4}\ \right] + \frac{u_5yz}{\eta_4} - \frac{u_5u_9}{u_8}z$$

Further computation gives:

$$\frac{dN_2}{dt} \leq -u_4\left[1 - \frac{u_2\bar{y}\,(1+\bar{x})}{\bar{\eta}_1}\right](x-\bar{x})^2 - u_4(y-\bar{y})^2 - u_4\left[\frac{u_1}{\eta_2\bar{\eta}_2} + \frac{1}{\eta_1\eta_3} - \frac{1}{\eta_1\bar{\eta}_1\eta_3} + \frac{u_2x\bar{x}}{\eta_1\bar{\eta}_1\eta_3}\right](x-\bar{x})(y-\bar{y}) - \left[\frac{u_5u_9}{u_8} - \frac{u_3\,u_4\bar{y}}{\bar{\eta}_1} - u_5\bar{y}\right]z + u_4(y-\bar{y})^2$$

Consequently, using the conditions (21a) and (21b) yield that:

$$\frac{dN_2}{dt} \leq -u_4\left[\sqrt{1 - \frac{u_2\bar{y}(1+\bar{x})}{\bar{\eta}_1}}(x-\bar{x}) + (y-\bar{y})\right]^2 - \left[\frac{u_5u_9}{u_8} - \frac{u_3\,u_4\bar{y}}{\bar{\eta}_1} - u_5\bar{y}\right]z + u_4(y-\bar{y})^2.$$

Accordingly, with the help of condition (21c), it is observed that $\frac{dN_2}{dt}$ is negative definite and hence all the trajectories stating from points satisfy the given conditions approach asymptotically to TPFEP. ■

Theorem (6): Assume that the CEP is locally asymptotically stable, then all the trajectories of the system (2) starting from points belong to the sub-region of $\mathbb{R}_+{}^3$, which satisfy the following sufficient conditions, approach asymptotically to CEP.

$$q_{12}{}^2 < q_{11}q_{22}, \tag{22a}$$

$$q_{13}{}^2 < q_{11}, \tag{22b}$$

$$q_{23}{}^2 < q_{22}, \tag{22c}$$

$$\frac{u_2y^*(x+x^*)}{\eta_1\eta_{1*}\eta_{3*}} < 1, \tag{22d}$$

$$2q_{22}(y-y^*)^2 < \frac{1}{2}\left[\sqrt{q_{11}}\,(x-x^*) + \sqrt{q_{22}}(y-y^*)\right]^2, \tag{22e}$$

$$(z-z^*) < \frac{1}{2}\left[\sqrt{q_{22}}\,(y-y^*) + (z-z^*)\,\right]^2, \tag{22f}$$

where the symbols $q_{ij}, i,j = 1,2,3$ are given in the proof.

Proof: Consider the following real valued function:

$$N_3(x,y,z) = \left(x - x^* - x^* \ln\left(\frac{x}{x^*}\right)\right) + \left(y - y^* - y^* \ln\left(\frac{y}{y^*}\right)\right) + \left(z - z^* - z^* \ln\left(\frac{z}{z^*}\right)\right)$$

Clearly the function N_3 is a positive definite function, that is $N_3(x^*,y^*,z^*) = 0$, while $N_3(x,y,z) > 0$, for all values in the region $\{(x,y,z) \in \mathbb{R}_+{}^3 : x > 0, y > 0, z > 0;\ (x,y,z) \neq (x^*,y^*,z^*)\}$. Thus after some algebraic manipulation it is obtain that:

$$\frac{dN_3}{dt} = -\frac{q_{11}}{2}(x-x^*)^2 - q_{12}(x-x^*)(y-y^*) - \frac{q_{22}}{2}(y-y^*)^2 + 2q_{22}(y-y^*)^2 + q_{13}(x-x^*)(z-z^*) - q_{23}(y-y^*)(z-z^*) \pm (z-z^*)^2,$$

Where

$$q_{11} = 1 - \frac{u_2 y^*(x+x^*)}{\eta_1\eta_{1_*}\eta_3},\ q_{22} = \frac{u_5 u_6 z^*(y+y^*)}{\eta_4\eta_{4_*}},\ q_{13} = \frac{u_3 y^*}{\eta_1\eta_3\eta_{3_*}},$$

$$q_{12} = \frac{u_1}{\eta_2\eta_{2_*}} + \frac{1}{\eta_1\eta_3} - \frac{u_4(1-u_2x^*x)}{\eta_1\eta_{1_*}\eta_{3*}},\ q_{23} = \frac{u_3u_4x^*(1+u_2x^*x)}{\eta_1\eta_{1_*}\eta_3\eta_{3_*}} + \frac{u_5}{\eta_4} + \frac{u_8(1-u_6yy^*)}{\eta_4\eta_{4_*}}.$$

Consequently, using the conditions (22a)-(22d) gives

$$\frac{dN_3}{dt} \leq -\frac{1}{2}\left[\sqrt{q_{11}}\,(x-x^*) + \sqrt{q_{22}}(y-y^*)\right]^2 + 2q_{22}(y-y^*)^2 - \frac{1}{2}\left[\sqrt{q_{22}}\,(y-y^*) + (z-z^*)\,\right]^2 + (z-z^*) - \frac{1}{2}\left[\sqrt{q_{11}}\,(x-x^*) - (z-z^*)\right]^2.$$

Clearly, with the help of conditions (22e), and (22f), it is observed that $\frac{dN_2}{dt}$ is negative definite and hence all the trajectories stating from points satisfy the given conditions approach asymptotically to CEP.

6. BIFURCATION ANALYSIS

In this section, an investigation of the effect of varying the values of the parameters on the system's dynamical behavior (2) is carried out using Sotomayor's theorem for local bifurcation. Recall that,

the non-hyperbolic equilibrium point of the dynamical system is a necessary but not sufficient condition for a bifurcation to occur. Therefore, the parameter that makes the equilibrium point a non-hyperbolic point is chosen as a candidate bifurcation parameter.

Rewrite the system (2) in the form

$$\frac{dX}{dt} = F(X),\ X = (x, y, z)^T,\ F = (xf_1, yf_2, zf_3)^T. \tag{23}$$

Also, the second directional derivative of the right hand side of the system (2) can be determined as:

$$D^2F(X, \mu)(W, W) = [d_{i1}]_{3x1}, \tag{24}$$

where $W = (w_1, w_2, w_3)^T$ be any non-zero vector and μ is any parameter, with

$$d_{11} = \left[-2 + \frac{2u_2xy(3-u_2x^2)}{\eta_1^3\eta_3}\right] w_1^2 - 2\left[\frac{u_1}{\eta_2^2} + \frac{(1-u_2x^2)}{\eta_1^2\eta_3}\right] w_1w_2 + 2\frac{u_3(1-u_2x^2)y}{\eta_1^2\eta_3^2} w_1w_3 + 2\frac{u_3x}{\eta_1\eta_3^2} w_2w_3 + 2\frac{{u_1}^2x}{\eta_2^3}w_2^2 - 2\frac{{u_3}^2xy}{\eta_1\eta_3^3}w_3^2,$$

$$d_{21} = -2\frac{u_2u_4xy(3-u_2x^2)}{\eta_1^3\eta_3}w_1^2 + 2\frac{u_4(1-u_2x^2)}{\eta_1^2\eta_3} w_1w_2 - 2\frac{u_3u_4(1-u_2x^2)y}{\eta_1^2\eta_3^2} w_1w_3 - 2\left[\frac{u_5(1-u_6y^2)}{\eta_4^2} + \frac{u_3u_4x}{\eta_1\eta_3^2}\right] w_2w_3 + 2\frac{u_5u_6yz(3-u_6y^2)}{\eta_4^3}w_2^2 + 2\frac{u_3^2u_4xy}{\eta_1\eta_3^3}w_3^2,$$

$$d_{31} = -2\frac{u_6u_8zy(3-u_6y^2)}{\eta_4^3}w_2^2 + 2\frac{u_8(1-u_6y^2)}{\eta_4^2} w_2w_3$$

According to the above calculation, the following theorems investigate the possibility of occurrence of local bifurcation in the system (2).

Theorem (7): Assume that the following condition holds, then the system (2) at the AEP undergoes a transcritical bifurcation when the parameter u_7 passes through the value $u_7^* = \frac{u_4}{1+u_2}$.

$$1 \neq u_2, \tag{25}$$

Proof: The Jacobian matrix of the system (2) at (e_1, u_7^*) can be written as:

$$J_1 = J(e_1, u_7^*) = \begin{pmatrix} -1 & -u_1 - \frac{1}{1+u_2} & 0 \\ 0 & 0 & 0 \\ 0 & 0 & -u_9 \end{pmatrix},$$

Then the matrix J_1 have two eigenvalues with negative real parts, and the third one is zero, say

$\lambda_{12}{}^{*} = 0$. Hence e_1 is non-hyperbolic point.

Let $\theta_1 = (\theta_{11}, \theta_{12}, \theta_{13})^T$ be the eigenvector corresponding to the eigenvalue $\lambda_{12}{}^{*} = 0$. Thus, $J_1\theta_1 = 0$, gives that $\theta_1 = (\sigma_1\theta_{12}, \theta_{12}, 0)^T$, where $\sigma_1 = -\left(u_1 + \frac{1}{1+u_2}\right)$, and $\theta_{12} \neq 0$ any real number.

Now, let $\Upsilon_1 = (\gamma_{11}, \gamma_{12}, \gamma_{13})^T$ represents the eigenvector corresponding to the eigenvalue $\lambda_{12}{}^{*} = 0$ of the matrix $J_1{}^T$. Thus, $J_1{}^T\Upsilon_1 = 0$ gives that $\Upsilon_1 = (0, \gamma_{12}, 0)^T$, where $\gamma_{12} \neq 0$ any real number. Now, according to the Sotomoyar's theorem, it is obtain that:

$$\frac{\partial F}{\partial u_7} = F_{u_7}(X, u_7) = (0, -\mathrm{y}, 0)^T \implies \frac{\partial F}{\partial u_7} = F_{u_7}(e_1, u_7^*) = (0, 0, 0)^T.$$

Therefore, $\Upsilon_1{}^T F_{u_7}(e_1, u_7^*) = 0$, hence the system (2) has no saddle-node bifurcation. Moreover, since

$$DF_{u_7}(X, u_7) = \begin{pmatrix} 0 & 0 & 0 \\ 0 & -1 & 0 \\ 0 & 0 & 0 \end{pmatrix} \implies DF_{u_7}(e_1, u_7^*)\theta_1 = (0, -\theta_{12}, 0)^T.$$

Then, $\Upsilon_1{}^T DF_{u_7}(e_1, u_7^*)\theta_1 = -\theta_{12}\gamma_{12} \neq 0$.

Also, by using equation (24), it is obtain that:

$$D^2F(e_1, u_7^*)(\theta_1, \theta_1) = \begin{pmatrix} [-2]\sigma_1{}^2\theta_{12}{}^2 - 2\left[u_1 + \frac{(1-u_2)}{(1+u_2)^2}\right]\sigma_1\theta_{12}{}^2 + 2u_1{}^2\theta_{12}{}^2 \\ 2\frac{u_4(1-u_2)}{(1+u_2)^2}\,\sigma_1\theta_{12}{}^2 \\ 0 \end{pmatrix}.$$

Then, due to condition (25) it is observed that:

$$\Upsilon_1{}^T D^2F(e_1, u_7^*)(\theta_1, \theta_1) = \frac{2u_4(1-u_2)}{1+u_2}\,\sigma_1\theta_{12}{}^2\gamma_{12} \neq 0.$$

Then a transcrtical bifurcation take place in the sense of Sotomayor. ■

Theorem (8): Assume that the conditions (13a) and (13b) together with the following condition hold. Then the system (2) at the TPFEP undergoes a transcritical bifurcation when the parameter u_9 passes through the value $u_9^* = \frac{u_8\bar{y}}{\bar{\eta}_4}$.

$$(1 - u_6\bar{y}^2)\,\sigma_3 \neq 0, \tag{26}$$

where the symbol σ_3 is given in the proof.

Proof: The Jacobian matrix of the system (2) at (e_2, u_9^*) can be written as:

$$J_2 = J(e_2, u_9^*) = \begin{pmatrix} b_{11} & b_{12} & b_{13} \\ b_{21} & 0 & b_{23} \\ 0 & 0 & 0 \end{pmatrix},$$

where $b_{ij}, i = 1,2 \; and \; j = 1,2,3$ are given in Eq. (11a). Clearly, e_2 becomes a non-hyperbolic point at $u_9 = u_9^*$, due to existence of zero eigenvalue, say ${\lambda_{23}}^* = 0$, while the other two eigenvalues λ_{21}, and λ_{22} are given in Eq. (12) and having negative real parts under the conditions (13a) and (13b).

Let $\theta_2 = (\theta_{21}, \theta_{22}, \theta_{23})^T$ be the eigenvector corresponding to the eigenvalue ${\lambda_{23}}^* = 0$. Thus, $J_2\theta_2 = 0$, gives that $\theta_2 = (\sigma_2\theta_{23}, \sigma_3\theta_{23}, \theta_{23})^T$, where $\sigma_2 = \frac{-b_{23}}{b_{21}}$, $\sigma_3 = \frac{b_{11}b_{23} - b_{13}b_{21}}{b_{21}b_{12}}$, $\theta_{23} \neq 0$ any real number.

Now, let $\Upsilon_2 = (\gamma_{21}, \gamma_{22}, \gamma_{23})^T$ represents the eigenvector corresponding to the eigenvalue ${\lambda_{23}}^* = 0$ of the matrix ${J_2}^T$. Thus, ${J_2}^T\Upsilon_2 = 0$ gives that $\Upsilon_2 = (0,0, \gamma_{23})^T$, where $\gamma_{23} \neq 0$ any real number. Now, since:

$$\frac{\partial F}{\partial u_9} = F_{u_9}(X, u_9) = (0, 0, -z)^T \Rightarrow \frac{\partial F}{\partial u_7} = F_{u_9}(e_2, u_9^*) = (0, 0, 0)^T.$$

Therefore, ${\Upsilon_2}^T F_{u_9}(e_2, u_9^*) = 0$, hence the system (2) has no saddle-node bifurcation. Moreover, since

$$DF_{u_9}(X, u_9^*) = \begin{pmatrix} 0 & 0 & 0 \\ 0 & 0 & 0 \\ 0 & 0 & -1 \end{pmatrix} \Rightarrow DF_{u_9}(e_2, u_9^*)\theta_2 = (0, 0, -\theta_{23})^T.$$

Then, ${\Upsilon_2}^T DF_{u_9}(e_2, u_9^*)\theta_2 = -\theta_{23}\gamma_{23} \neq 0$.

Also, by using equation (24), it is obtain that:

$$D^2F(e_2, \alpha_9^*)(\theta_2, \theta_2) = [\bar{d}_{i1}]_{3\times 1},$$

Where

$$\bar{d}_{11} = \left[-2 + \frac{2u_2\bar{x}\bar{y}(3 - u_2\bar{x}^2)}{\bar{\eta}_1^3}\right](\sigma_2\theta_{23})^2 - 2\left[\frac{u_1}{\bar{\eta}_2^2} + \frac{(1 - u_2\bar{x}^2)}{\bar{\eta}_1^2}\right]\sigma_2\sigma_3{\theta_{23}}^2 + 2\frac{u_3(1 - u_2\bar{x}^2)\bar{y}}{\bar{\eta}_1^2}\sigma_2{\theta_{23}}^2 + 2\frac{u_3\bar{x}}{\bar{\eta}_1}\sigma_3{\theta_{23}}^2 + 2\frac{{u_1}^2\bar{x}}{\eta_2^3}(\sigma_3\theta_{23})^2 - 2\frac{{u_3}^2\bar{x}\bar{y}}{\bar{\eta}_1}{\theta_{23}}^2 \quad ,$$

$$\bar{d}_{21} = -2\frac{u_2u_4\bar{x}\bar{y}(3-u_2\bar{x}^2)}{\bar{\eta}_1^3}(\sigma_2\theta_{23})^2 + 2\frac{u_4(1-u_2\bar{x}^2)}{\bar{\eta}_1^2}\,\sigma_2\sigma_3{\theta_{23}}^2$$
$$-2\frac{u_3u_4(1-u_2\bar{x}^2)\bar{y}}{\bar{\eta}_1^2}\,\sigma_2{\theta_{23}}^2 - 2\left[\frac{u_5(1-u_6\bar{y}^2)}{\bar{\eta}_4^2} + \frac{u_3u_4\bar{x}}{\bar{\eta}_1}\right]\sigma_3{\theta_{23}}^2 + 2\frac{u_3^2u_4\bar{x}\bar{y}}{\bar{\eta}_1}{\theta_{23}}^2 \quad ,$$

$$\bar{d}_{31} = 2\frac{u_8(1-u_6\bar{y}^2)}{\bar{\eta}_4^2}\,\sigma_3{\theta_{23}}^2.$$

Then, using the conditions (26) yields:

$${\Upsilon_2}^T D^2F(e_2,u_9^*)(\theta_2,\theta_2) = \frac{2u_8(1-u_6\bar{y}^2)}{\bar{\eta}_4^2}\,\sigma_3(\theta_{23})^2\gamma_{23} \neq 0.$$

Hence a transcrtical bifurcation take place in the sense of Sotomayor. ■

Theorem (9): Assume that the conditions (16a), (16b), (16c), and (16e) together with the following condition hold. Then the system (2) at the CEP undergoes a saddle-node bifurcation when the parameter u_4 passes through the value $u_4^* = \frac{u_5\eta_{1*}\eta_{3*}^2[\eta_{1*}^2\eta_{3*}-2u_2x^*y^*]}{u_3\eta_{4*}[(1-u_2x^{*2})y^*-[\eta_{1*}^2\eta_{3*}-2u_2x^*y^*]x^*]}$.

$$\sigma_5\gamma_{32}{d_{11}}^* + \gamma_{32}{d_{21}}^* \neq 0, \tag{27}$$

Proof: The Jacobian matrix of the system (2) at CEP with $u_4 = u_4^*$ can be written as:

$$J_3 = J(e_3,u_4^*) = \begin{pmatrix} c_{11} & c_{12} & c_{13} \\ {c_{21}}^* & c_{22} & {c_{23}}^* \\ 0 & c_{32} & 0 \end{pmatrix},$$

where $c_{ij}, i,j = 1,2,3$ with ${c_{21}}^* = c_{21}(u_4^*)$, and ${c_{23}}^* = c_{23}(u_4^*)$. Direct computation shows that $c_{11}{c_{23}}^* - c_{13}{c_{21}}^* = 0$, hence the determinant of the matrix J_3 is equal to zero. Therefore the matrix J_3 has a zero eigenvalue given by ${\lambda_3}^* = 0$, and hence the CEP is a non-hyperbolic point. Let $\theta_3 = (\theta_{31},\theta_{32},\theta_{33})^T$ be the eigenvector corresponding to the eigenvalue ${\lambda_3}^* = 0$. Thus, $J_3\theta_3 = 0$, gives that $\theta_3 = (\sigma_4\theta_{33},0,\theta_{33})^T$, where, $\sigma_4 = -\frac{c_{13}}{c_{11}} > 0$ due to condition (16c), and $\theta_{33} \neq 0$ is any real number.

Now, let $\Upsilon_3 = (\gamma_{31},\gamma_{32},\gamma_{33})^T$ represents the eigenvector corresponding to the eigenvalue ${\lambda_3}^* = 0$ of the matrix ${J_3}^T$. Thus, ${J_3}^T\Upsilon_3 = 0$, gives that $\Upsilon_3 = (\sigma_5\gamma_{32},\gamma_{32},\sigma_6\gamma_{32})^T$, where $\sigma_5 = -\frac{c_{21}}{c_{11}} > 0$ due condition (16a), and $\sigma_6 = \frac{c_{12}c_{21}-c_{11}c_{22}}{c_{21}c_{32}} < 0$ due to conditions (16a), (16b), and (16e) with $\gamma_{32} \neq 0$ be any real number. Moreover, it is observed that:

$$\frac{\partial F}{\partial u_4} = F_{u_4}(X,u_4) = (0,\frac{x}{\eta_1\eta_3},0)^T \implies F_{u_4}(e_3,u_4^*) = (0,\frac{x^*}{\eta_{1*}\eta_{3*}},0)^T.$$

Therefore, $\Upsilon_3{}^T F_{u_4}(e_3, u_4^*) = \frac{x^*}{\eta_{1*}\eta_{3*}}\gamma_{32} \neq 0$,

Moreover, since

$$D^2F(e_3, u_4^*)(\theta_3, \theta_3) = [d_{i1}{}^*]_{3\times 1},$$

where

$$d_{11}{}^* = \left[-2 + \frac{2u_2x^*y^*\left(3-u_2x^{*2}\right)}{\eta_{1*}^3\eta_{3*}}\right](\sigma_4\theta_{33})^2 + 2\frac{u_3(1-u_2x^{*2})y^*}{\eta_{1*}^2\eta_{3*}^2}\sigma_4\,\theta_{33}{}^2 - 2\frac{u_3{}^2x^*y^*}{\eta_{1*}\eta_{3*}^3}\theta_{33}{}^2,$$

$$d_{21}{}^* = -2\frac{u_2u_4x^*y^*\left(3-u_2x^{*2}\right)}{\eta_{1*}^3\eta_{3*}}(\sigma_4\theta_{33})^2 - 2\frac{u_3u_4(1-u_2x^{*2})y^*}{\eta_{1*}^2\eta_{3*}^2}\,\sigma_4\,\theta_{33}{}^2 + 2\frac{u_3^2u_4x^*y^*}{\eta_{1*}\eta_{3*}^3}\theta_{33}{}^2,$$

$$d_{31}{}^* = 0.$$

Therefore, using the condition (27), it is obtain that

$$\Upsilon_3{}^T D^2F(e_3, u_4^*)(\theta_3, \theta_3) = \sigma_5\gamma_{32}d_{11}{}^* + \gamma_{32}d_{21}{}^* \neq 0$$

Then a saddle-node bifurcation take place in the sense of Sotomayor.

7. HOPF BIFURCATION ANALYSIS

In this section, the possibility of occurrence of the Hopf bifurcation is investigated. Recall that the three-dimensional dynamical system undergoes a Hopf bifurcation around an equilibrium point provided that the Jacobian matrix at that equilibrium point has one negative eigenvalue with two complex conjugate eigenvalues having real part $Re(\lambda)$ satisfies that $Re(\lambda)|_{\theta=\widehat{\theta}} = 0$, and $\frac{d}{d\theta}Re(\lambda)|_{\theta=\widehat{\theta}} \neq 0$ (known as transversality condition), where θ is a bifurcation parameter.

Theorem (10): Assume that the conditions (16a)-(16d) and (16f) along with the following condition hold:

$$2u_5u_6y^*z^*(\eta_{1*}^2\eta_{3*} - 2u_2x^*y^*)\eta_{1*}\eta_{2*}^2\eta_{3*} > u_4(u_1\eta_{1*}\eta_{3*} + \eta_{2*}^2)\left(1-u_2x^{*2}\right)\eta_{4*}^2, \quad (28a)$$

$$A_3{}'(u_8^*) > \left(A_1(u_8^*)A_2(u_8^*)\right)', \quad (28b)$$

where $A_i; i = 1,2,3$ are the coefficients of the characteristic equation (15). Then system (2) undergoes a Hopf bifurcation near the CEP as the parameter u_8 passes through the value u_8^*, where $u_8^* = \frac{(c_{11}+c_{22})(c_{11}c_{22}-c_{12}c_{21})\eta_{4*}^2}{z^*(1-u_6y^*)(c_{22}c_{23}+c_{13}c_{21})}$, with $c_{ij}; i,j = 1,2,3$ are the elements of the Jacobian

matrix J_{e_3}.

Proof: According to the form of $\Delta = A_1A_2 - A_3$ given in equation (15), it is easy to verify that $\Delta = 0$ when $u_8 = u_8^*$, where $u_8^* > 0$ provided that the given conditions are satisfied. Therefore, it is obtain $A_1(u_8^*)A_2(u_8^*) = A_3(u_8^*)$. Consequently, the characteristic equation (15) at $u_8 = u_8^*$ becomes

$$P_3(\lambda) = (\lambda + A_1)(\lambda^2 + A_2) = 0, \tag{29}$$

where A_1, and A_2 are positive due to the given conditions. Now direct computation gives that the equation (29) has the following roots

$$\lambda_1 = -A_1 \quad \text{and} \quad \lambda_{2,3} = \pm i\sqrt{A_2}.$$

Therefore, the first condition of the Hopf bifurcation that is represented by the existence of pure imaginary complex conjugate eigenvalues is satisfied when $u_8 = u_8^*$. Now, in the neighborhood of u_8^*, the complex conjugate eigenvalues take the form $\lambda_{2,3} = \delta_1(u_8) \pm i\delta_2(u_8)$. Hence substituting $\lambda = \delta_1(u_8) + i\delta_2(u_8)$ in equation (29), and then take the derivative with respect to the bifurcation parameter u_8. After that compare the two sides of resulting equation and then equating their real and imaginary parts, we get

$$\begin{aligned} \psi(u_8){\delta_1}'(u_8) + \phi(u_8){\delta_2}'(u_8) &= -\Theta(u_8), \\ \phi(u_8){\delta_1}'(u_8) + \psi(u_8){\delta_2}'(u_8) &= -\Gamma(u_8), \end{aligned} \tag{30}$$

where

$$\begin{aligned} \psi(u_8) &= 3{\delta_1}^2(u_8) + 2A_1(u_8)\delta_1(u_8) + A_2(u_8) - 3{\delta_2}^2(u_8), \\ \phi(u_8) &= 6\delta_1(u_8)\delta_2(u_8) + 2A_1(u_8)\delta_2(u_8), \\ \Theta(u_8) &= {\delta_1}^2(u_8){A_1}'(u_8) + {A_2}'(u_8)\delta_1(u_8) + {A_3}'(u_8) - {A_1}'(u_8){\delta_2}^2(u_8), \\ \Gamma(u_8) &= 2\delta_1(u_8)\delta_2(u_8){A_1}'(u_8) + {A_2}'(u_8)\delta_2(u_8). \end{aligned}$$

Solving the linear system (30), we get

$$\begin{aligned} {\delta_1}'(u_8) &= \frac{d\delta_1(u_8)}{du_8} = -\frac{\Theta(u_8)\psi(u_8) + \Gamma(u_8)\phi(u_8)}{[\psi(u_8)]^2 + [\phi(u_8)]^2}, \\ {\delta_2}'(u_5) &= -\frac{\Gamma(u_8)\psi(u_8) - \Theta(u_8)\phi(u_8)}{[\psi(u_8)]^2 + [\phi(u_8)]^2}. \end{aligned} \tag{31}$$

Hence, the transversality condition is satisfied provided that $\Theta(u_8^*)\psi(u_8^*) + \Gamma(u_8^*)\phi(u_8^*) \neq 0$. Obviously, we have that $\delta_1(u_8^*) = 0$ and $\delta_2(u_8^*) = \sqrt{A_2(u_8^*)}$, then the coefficients of system (30) at $u_8 = u_8^*$ become:

$$\psi(u_8^*) = -2A_2(u_8^*),$$

$$\phi(u_8^*) = 2A_1(u_8^*)\sqrt{A_2(u_8^*)}\ ,$$

$$\Theta(u_8^*) = A_3{}'(u_8^*) - A_1{}'(u_8^*)A_2(u_8^*),$$

$$\Gamma(u_8^*) = A_2{}'(u_8^*)\sqrt{A_2(u_8^*)}.$$

Therefore,

$$\Theta(u_8^*)\psi(u_8^*) + \Gamma(u_8^*)\phi(u_8^*) = -2A_2(u_8^*)\left[A_3{}'(u_8^*) - \left(A_1{}'(u_8^*)A_2(u_8^*) + A_1(u_8^*)A_2{}'(u_8^*)\right)\right].$$

Hence, $\Theta(u_8^*)\psi(u_8^*) + \Gamma(u_8^*)\phi(u_8^*) \neq 0$ under the condition (28b), which gives $\delta_1{}'(u_8^*) > 0$. Thus system (2) undergoes Hopf bifurcation at $u_8 = u_8^*$.

8. NUMERICAL SIMULATION

In this section, the food chain system (2) is solved numerically using the hypothetical set of biologically feasible parameters values that given by (8). The objectives are to confirm the theoretical finding and understand the impact of varying the values of the parameters including the fear rates on the dynamical behavior of the system. The obtained numerical solution of the food chain system (2) is presented in different forms such as phase portrait, time sires, bifurcation diagrams, and Lyapunov exponent's bifurcation diagram using Matlab version R2013a. The numerical trajectory of system (2) using the parameters set (8) with the initial point (0.8, 0.7, 0.6) are drawn in Figure (2).

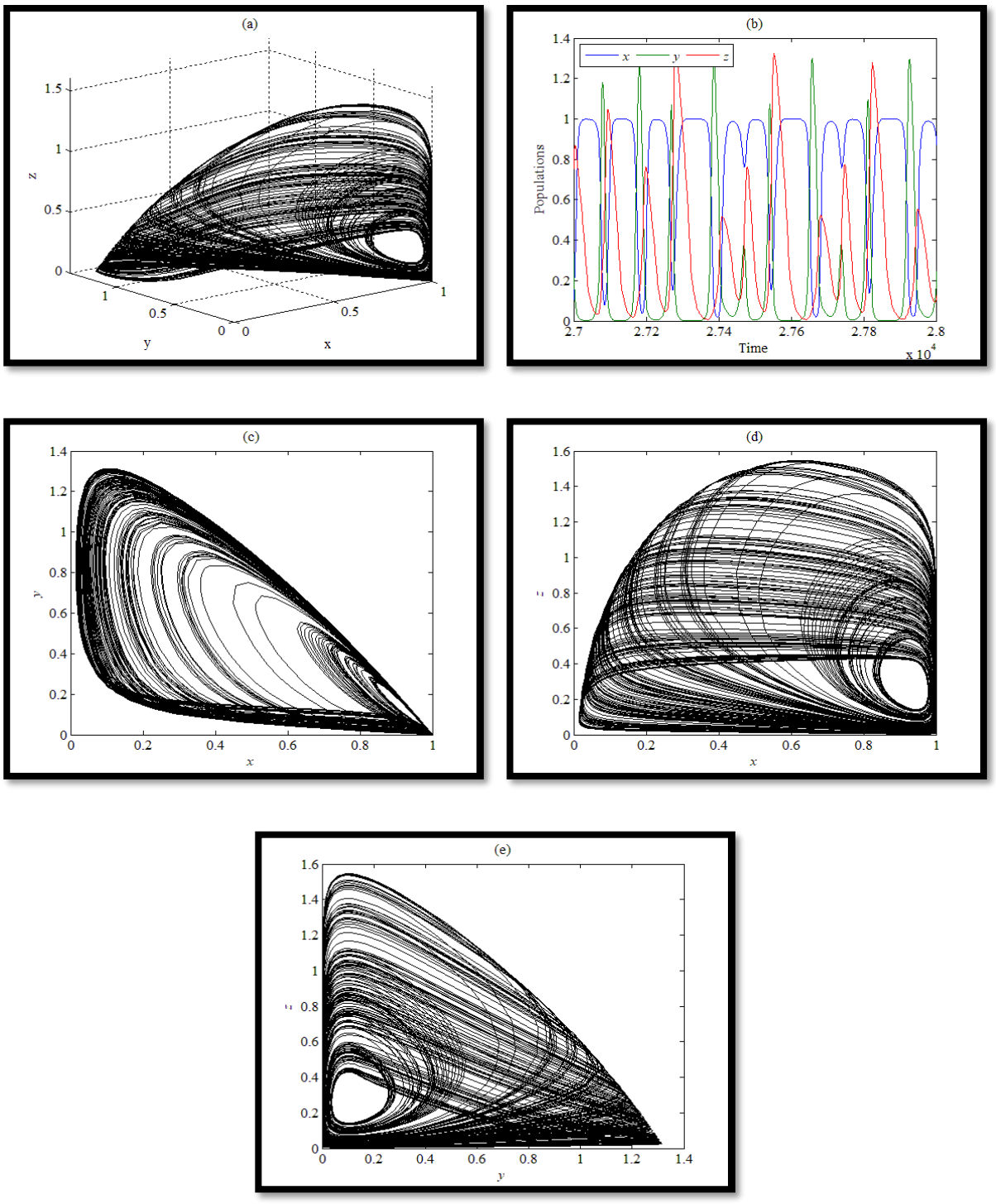

Figure 2. The trajectory of system (2) using parameters set (8). (a) 3D Phase portrait represents strange attractor. (b) Time sires of the strange attractor. (c) Projection of the strange attractor in the xy −plane. (d) Projection of the strange attractor in the xz −plane. (e) Projection of the strange attractor in the yz −plane.

According to Figure (2), system (2) approaches asymptotically to a strange attractor that was drawn after removing the transient effect. Now, the effect of varying the parameter u_1 in the range $[0, 1.5]$ on the dynamics of the system (2) is investigated numerically using the bifurcation diagram along with Lyapunov exponents bifurcation diagrams as shown in Figure (3).

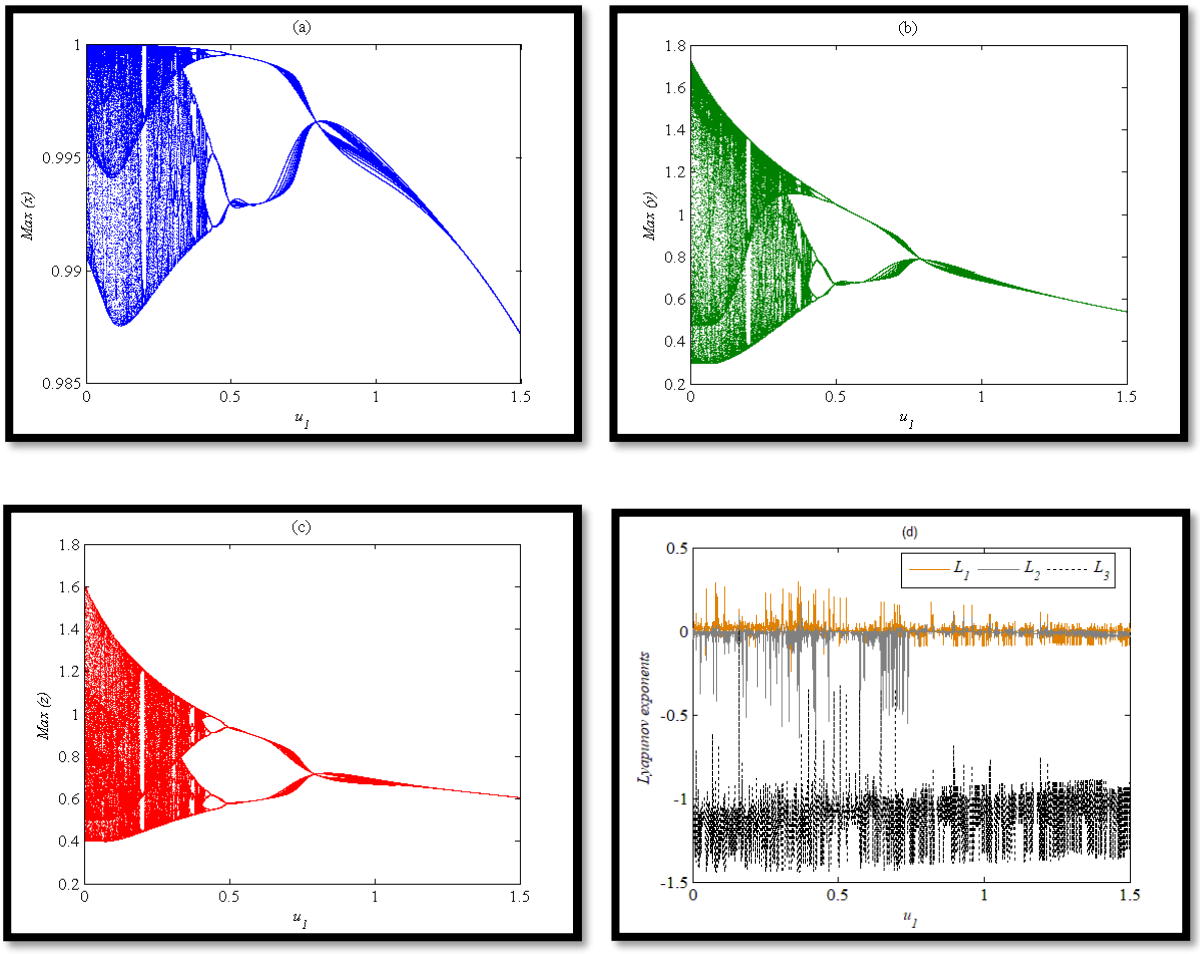

Figure 3. Bifurcation diagrams as a function of u_1. (a) *Max* (*x*) vs. u_1. (b) *Max* (*y*) vs. u_1. (c) *Max* (*z*) vs. u_1. (d) Lyapunov exponents vs. u_1.

According to Figure (3), the bifurcation diagrams show clearly the existence of chaos for the range $0 \leq u_1 \leq 1.05$. As the value of u_1 increases so that $1.06 \leq u_1 \leq 4.07$, the chaotic dynamics transfer to periodic dynamic as shown in Figure 4(a-b) for typical value of u_1, while the system (2) approaches asymptotically to a stable CEP for $4.08 \leq u_1 \leq 37$ as shown in the Figure 5(a-b) for a typical value of u_1. Furthermore, for $38 \leq u_1$ system (2) loses its persistence and

approaches asymptotically to TPFEP as shown in Figure 6(a-b) for typical value of u_1.

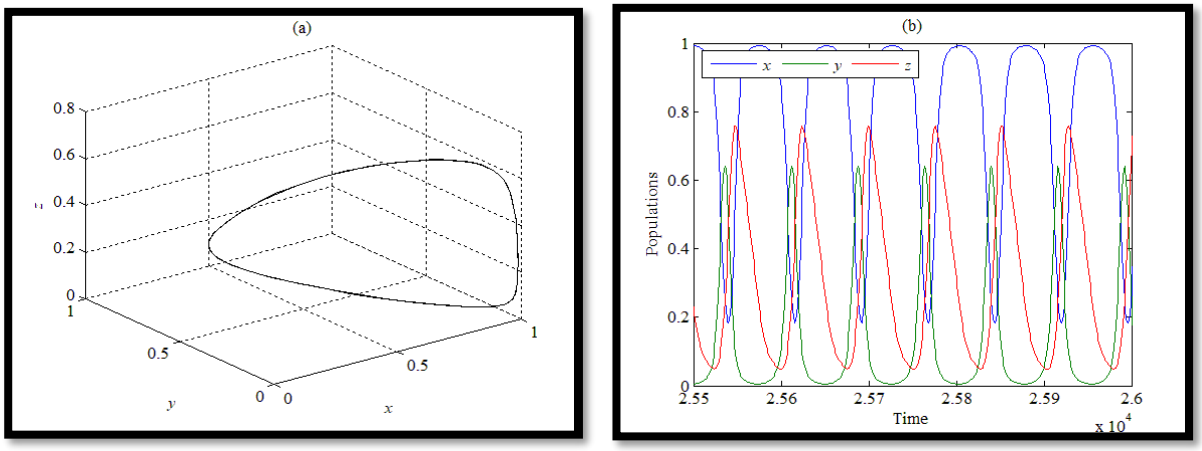

Figure 4. The trajectory of system (2) for the data (8) with $u_1 = 1.2$. (a) 3D periodic attractor. (b) Time series of the periodic attractor in (a).

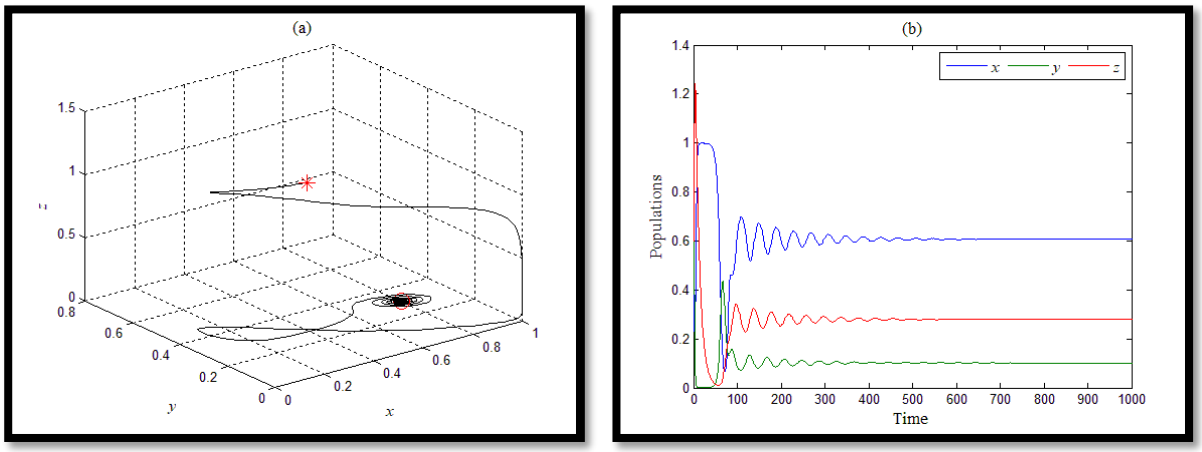

Figure 5. The trajectory of system (2) for the data (8) with $u_1 = 5$. (a) Asymptotically stable CEP that given by $(0.6,0.1,0.27)$. (b) Time series of the periodic attractor in (a).

The effect of varying the parameter u_2 in the range $[0.8, 2]$ on the dynamics of the system (2) is investigated numerically using the bifurcation diagram along with Lyapunov exponents bifurcation diagrams as shown in Figure (6).

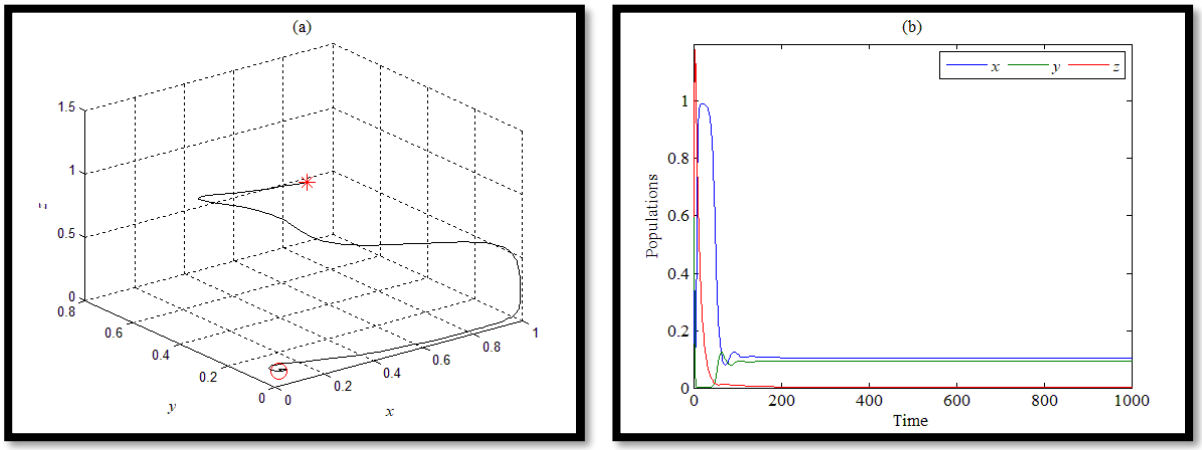

Figure 6. The trajectory of system (2) for the data (8) with $u_1 = 45$. (a) Asymptotically stable TPFEP that given by $(0.1,0.09,0)$. (b) Time series of the periodic attractor in (a).

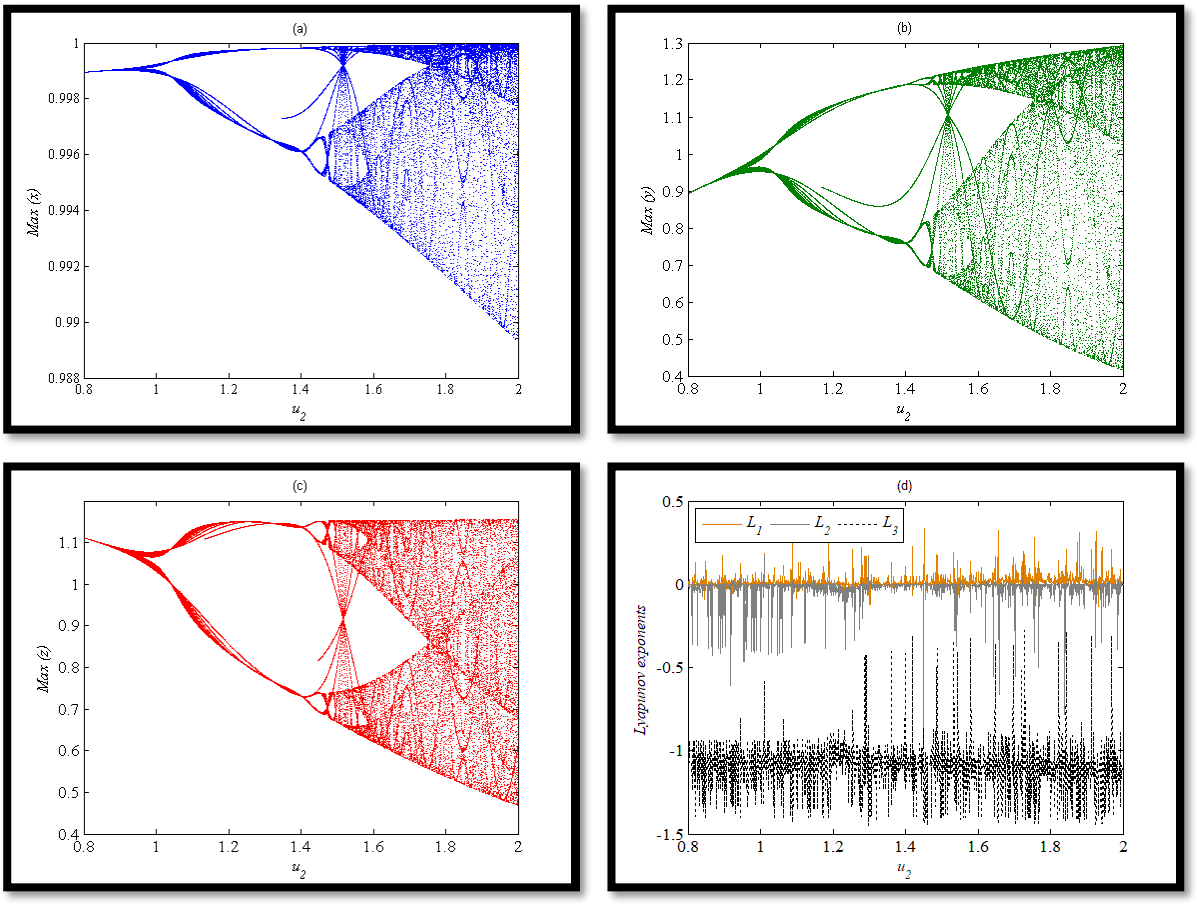

Figure 7. Bifurcation diagrams as a function of u_2. (a) *Max* (x) vs. u_2. (b) *Max* (y) vs. u_2. (c) *Max* (z) vs. u_2. (d) Lyapunov exponents vs. u_2.

Clearly, system (2) has complex dynamics including chaos as shown in Figure (7). It is observed that for the range $0.01 \leq u_2 \leq 0.4$ the system approaches asymptotically to CEP, however for the range $0.41 \leq u_2 \leq 0.8$, the system (2) has a periodic attractor, see Figures (8) and (9) for typical values of u_2. Further, an increase for the value of u_2 in the range $0.8 \leq u_2 < 9$ enters the system (2) to the complex dynamics region. However, for $9 \leq u_2$, the system (2) approaches asymptotically to AEP.

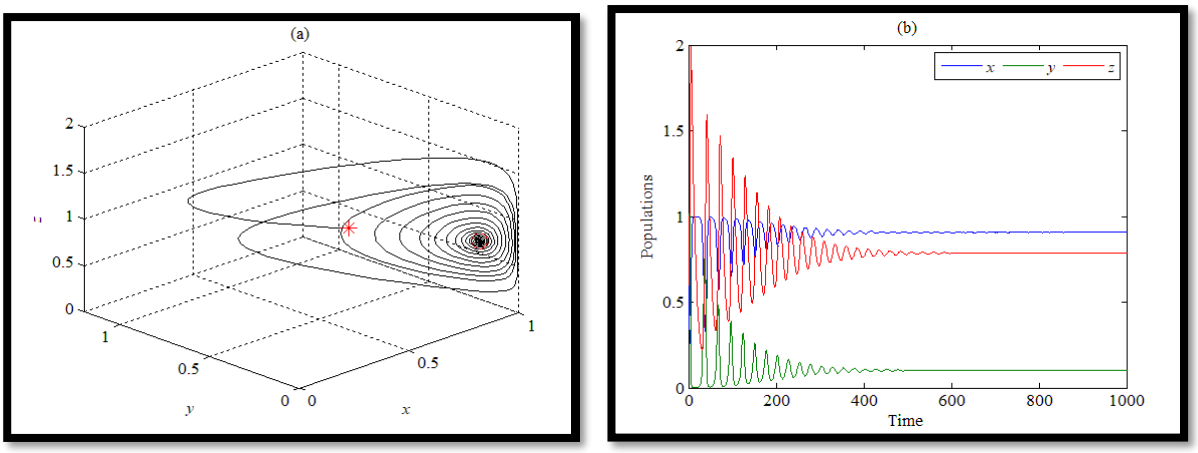

Figure 8. The trajectory of system (2) for the data (8) with $u_2 = 0.3$. (a) Asymptotically stable CEP that given by $(0.9,0.1,0.78)$. (b) Time series of the periodic attractor in (a).

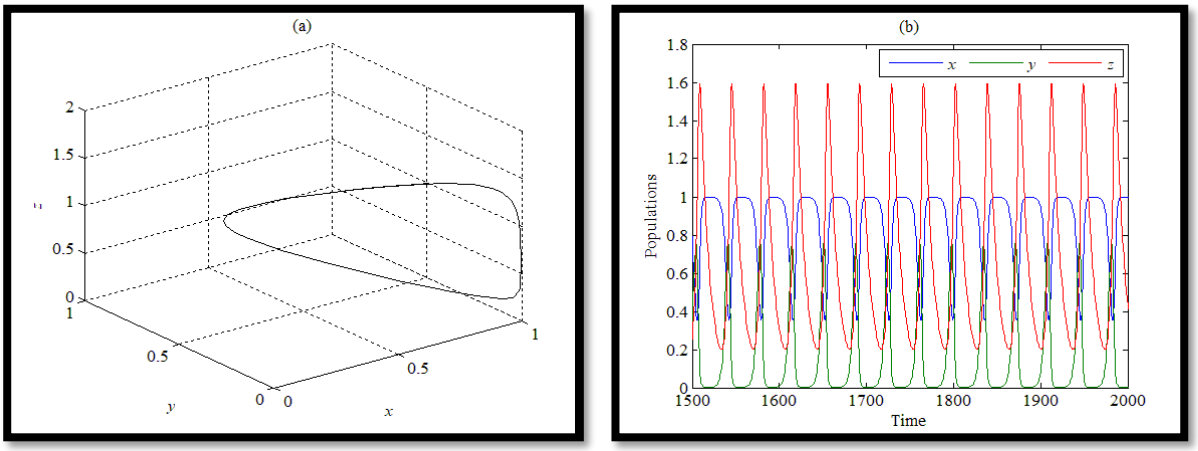

Figure 9. The trajectory of system (2) for the data (8) with $u_2 = 0.5$. (a) 3D periodic attractor. (b) Time series of the periodic attractor in (a).

The influence of the varying u_3 in the range $[0, 2]$, is presented in the bifurcation diagrams given by Figure (10). The trajectory of system (2) for the parameters set (8) with the $u_3 = 1.5$ is presented in Figure (11) too.

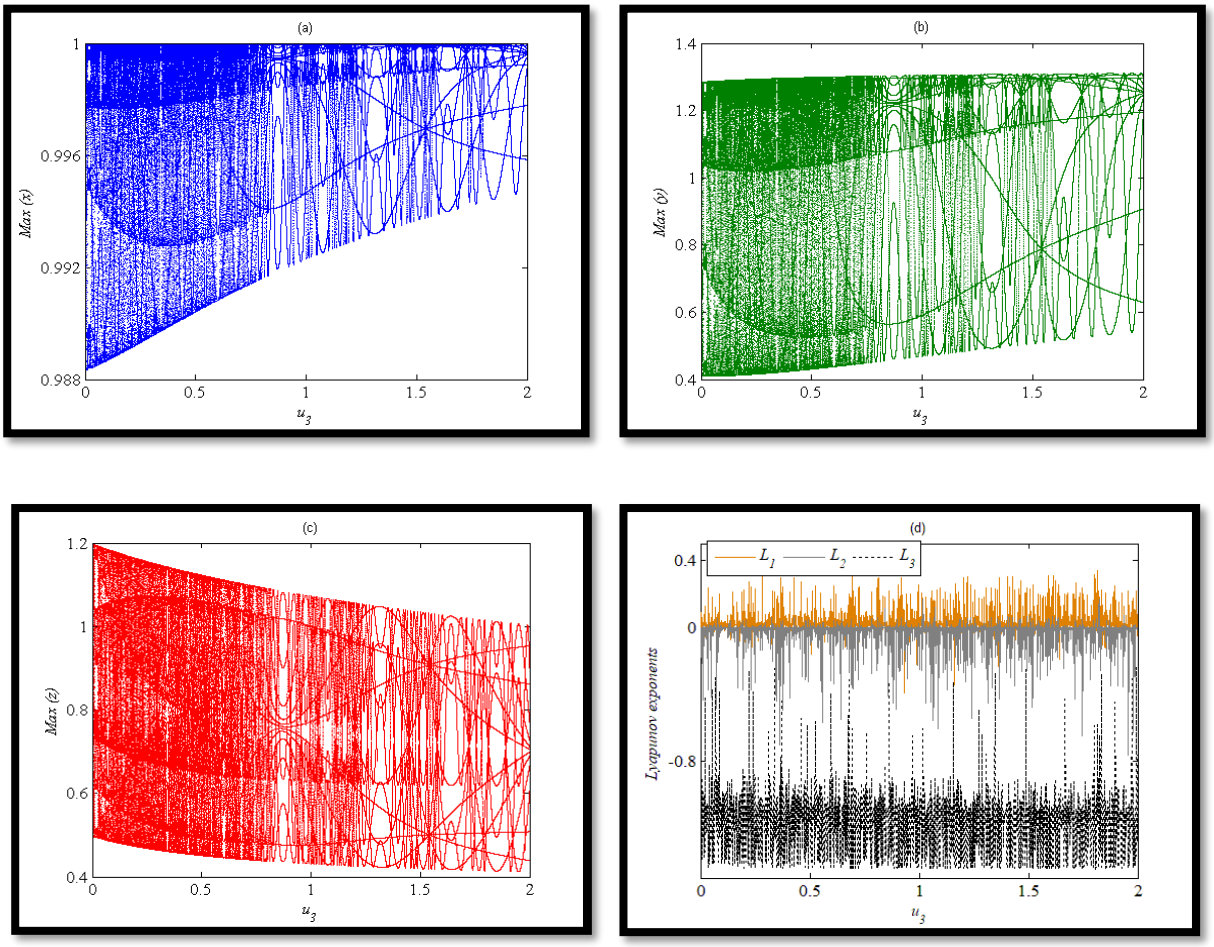

Figure 10. Bifurcation diagrams as a function of u_3. (a) *Max* (*x*) vs. u_3. (b) *Max* (*y*) vs. u_3. (c) *Max* (*z*) vs. u_3. (d) Lyapunov exponents vs. u_3.

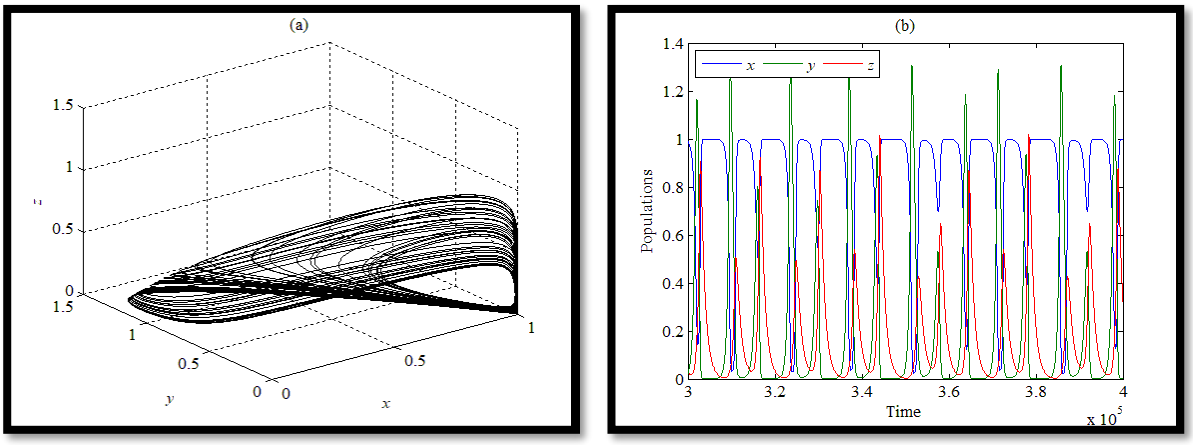

Figure 11. The trajectory of system (2) for the data (8) with $u_3 = 1.5$. (a) Strange attractor. (b) Time series of the strange attractor in (a).

Obviously, Figures (10) and (11) show the presence of complex dynamics including chaos for the wide range of the parameter u_3. The existence of a positive Lyapunov exponent throughout the range ensures the existence of chaos too.

Moreover, the impact of varying other parameters of the system (2) on its dynamical behavior is also investigated using bifurcation diagrams and Lyapunov exponents bifurcation diagrams, and the obtained results are presented in Figures (12)-(17) for the parameters u_4, u_5, u_6, u_7, u_8, and u_9 respectively.

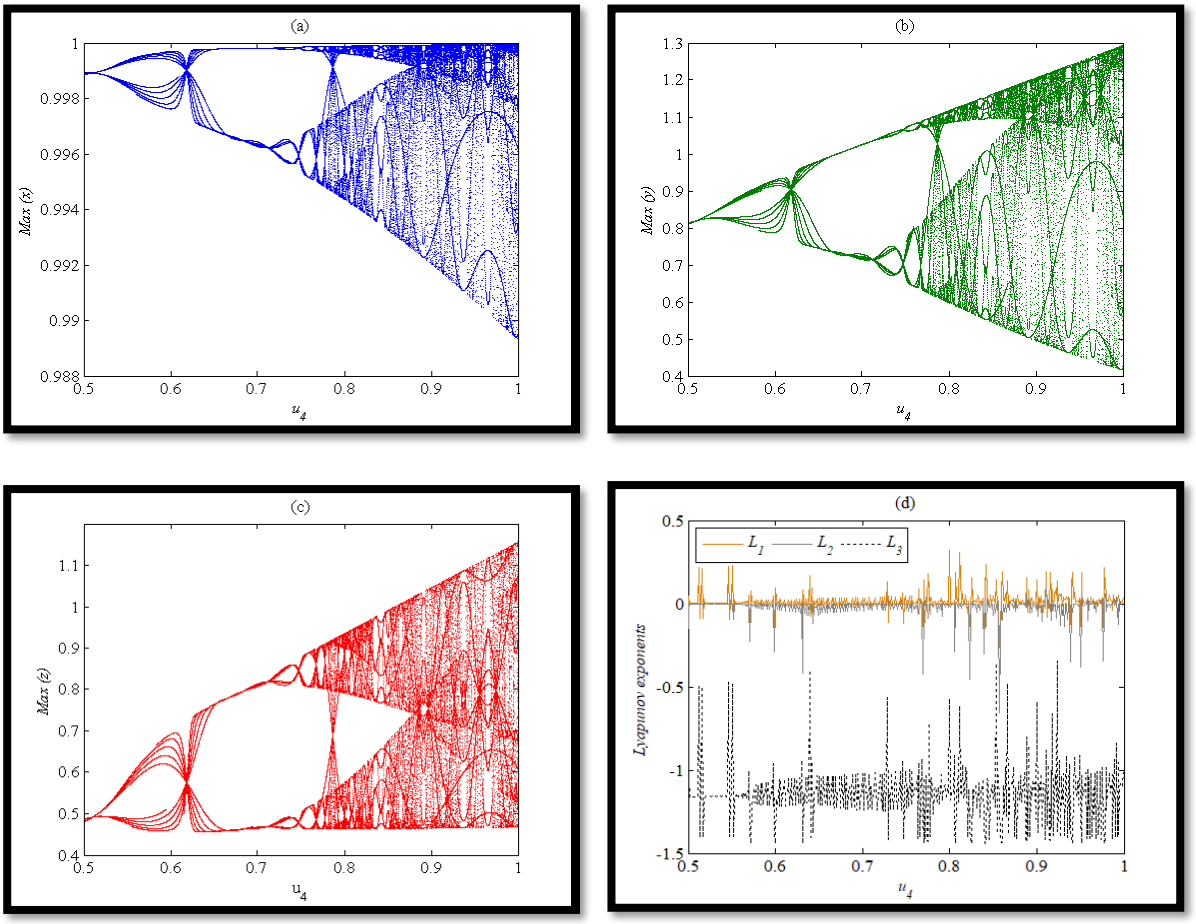

Figure 12. Bifurcation diagrams as a function of u_4. (a) *Max* (*x*) vs. u_4. (b) *Max* (*y*) vs. u_4. (c) *Max* (*z*) vs. u_4. (d) Lyapunov exponents vs. u_4.

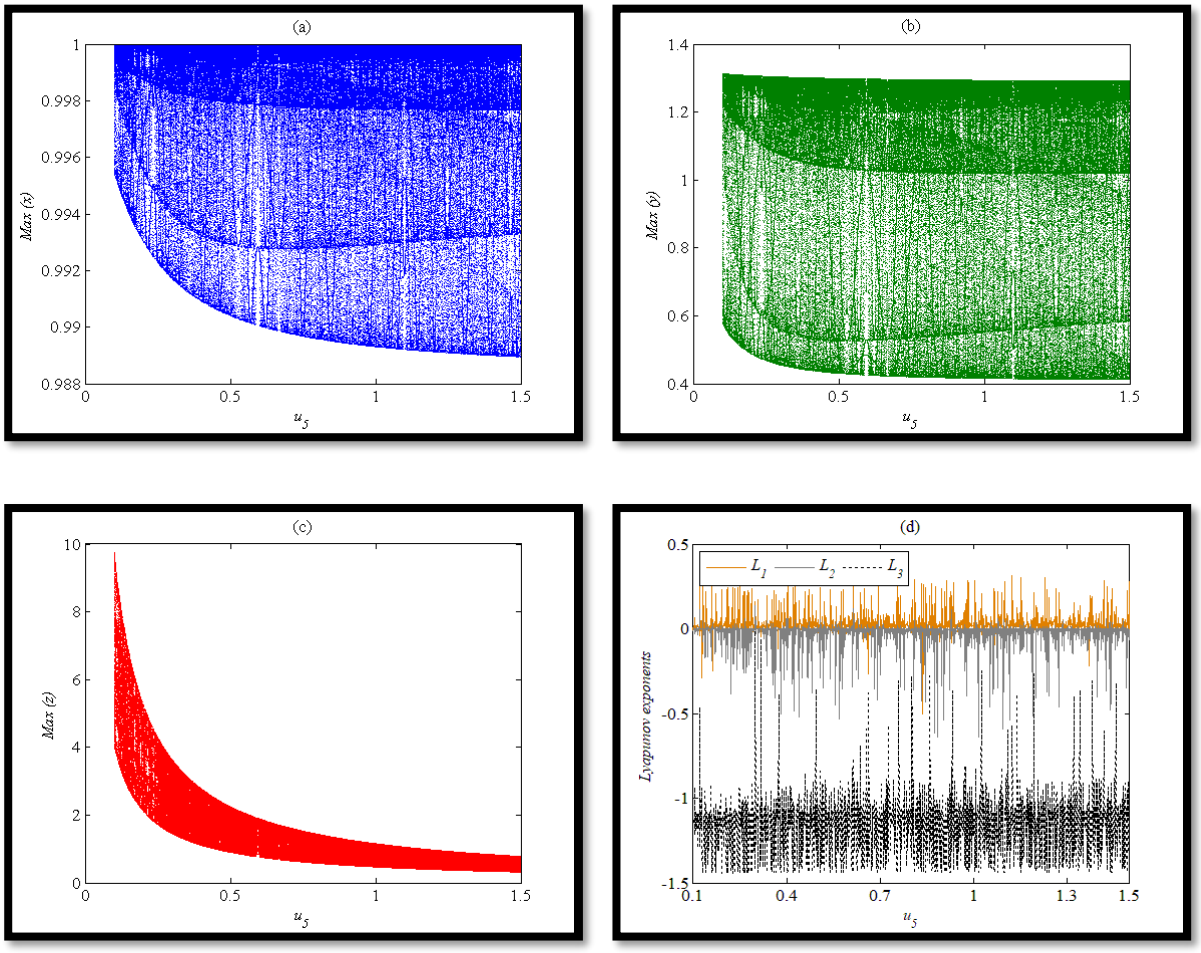

Figure 13. Bifurcation diagrams as a function of u_5. (a) *Max* (*x*) vs. u_5. (b) *Max* (*y*) vs. u_5. (c) *Max* (*z*) vs. u_5. (d) Lyapunov exponents vs. u_5.

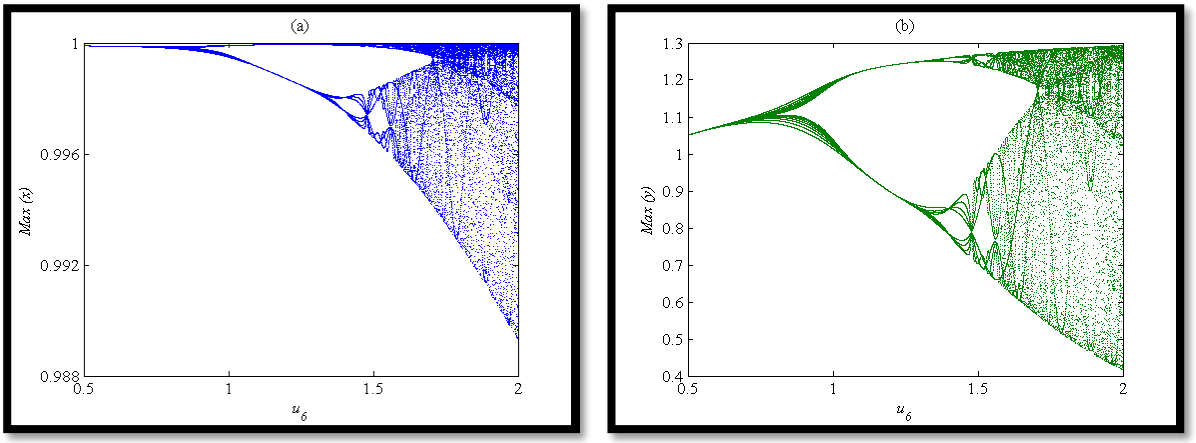

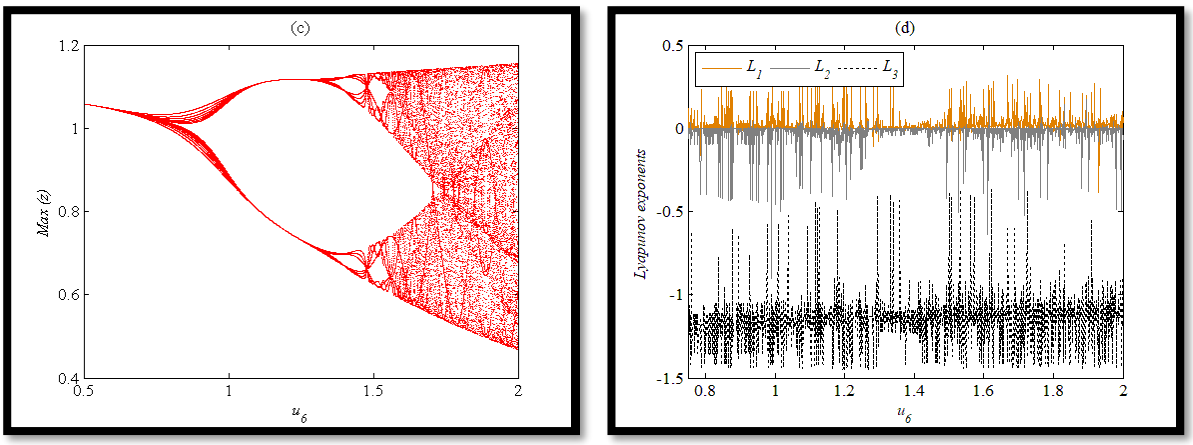

Figure 14. Bifurcation diagrams as a function of u_6. (a) *Max* (*x*) vs. u_6. (b) *Max* (*y*) vs. u_6. (c) *Max* (*z*) vs. u_6. (d) Lyapunov exponents vs. u_6.

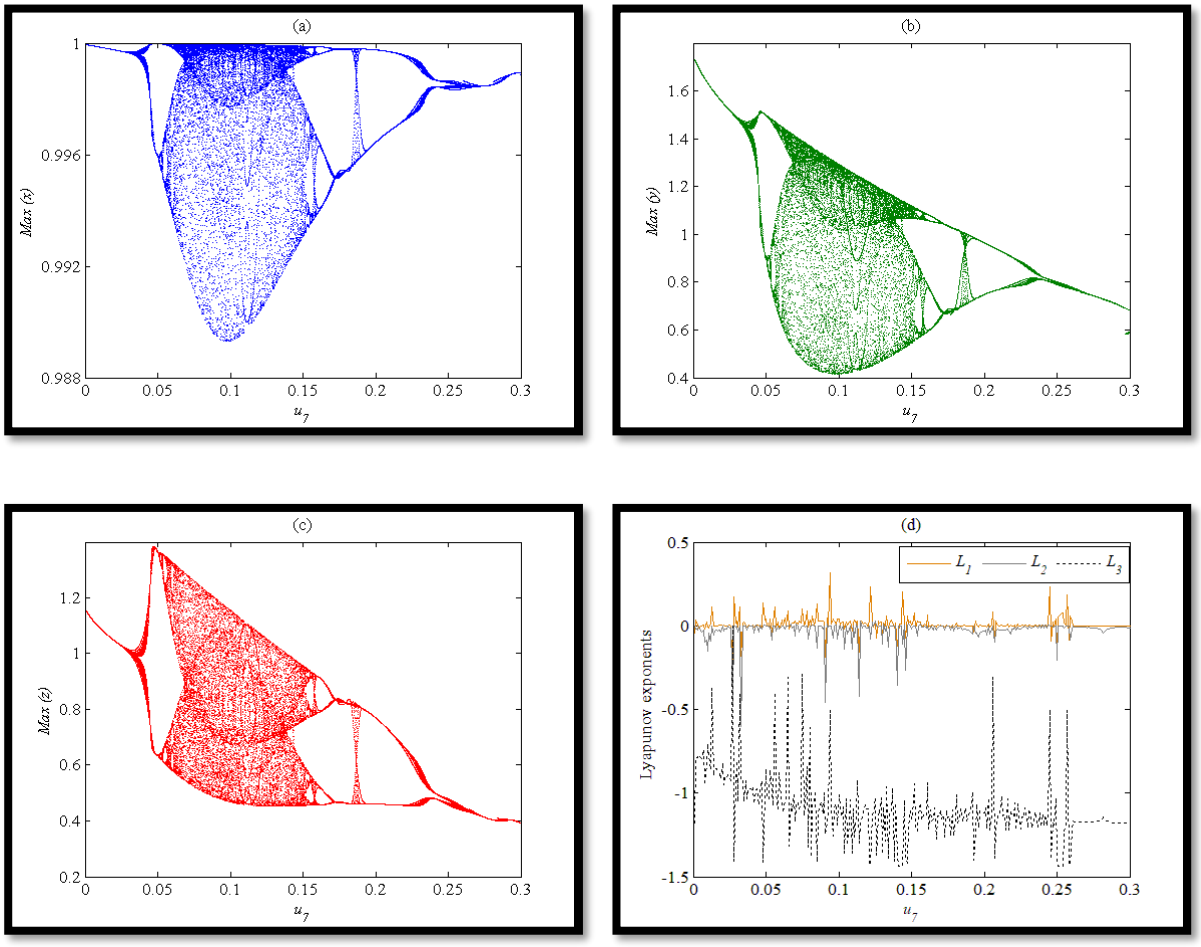

Figure 15. Bifurcation diagrams as a function of u_7. (a) *Max* (*x*) vs. u_7. (b) *Max* (*y*) vs. u_7. (c) *Max* (*z*) vs. u_7. (d) Lyapunov exponents vs. u_7.

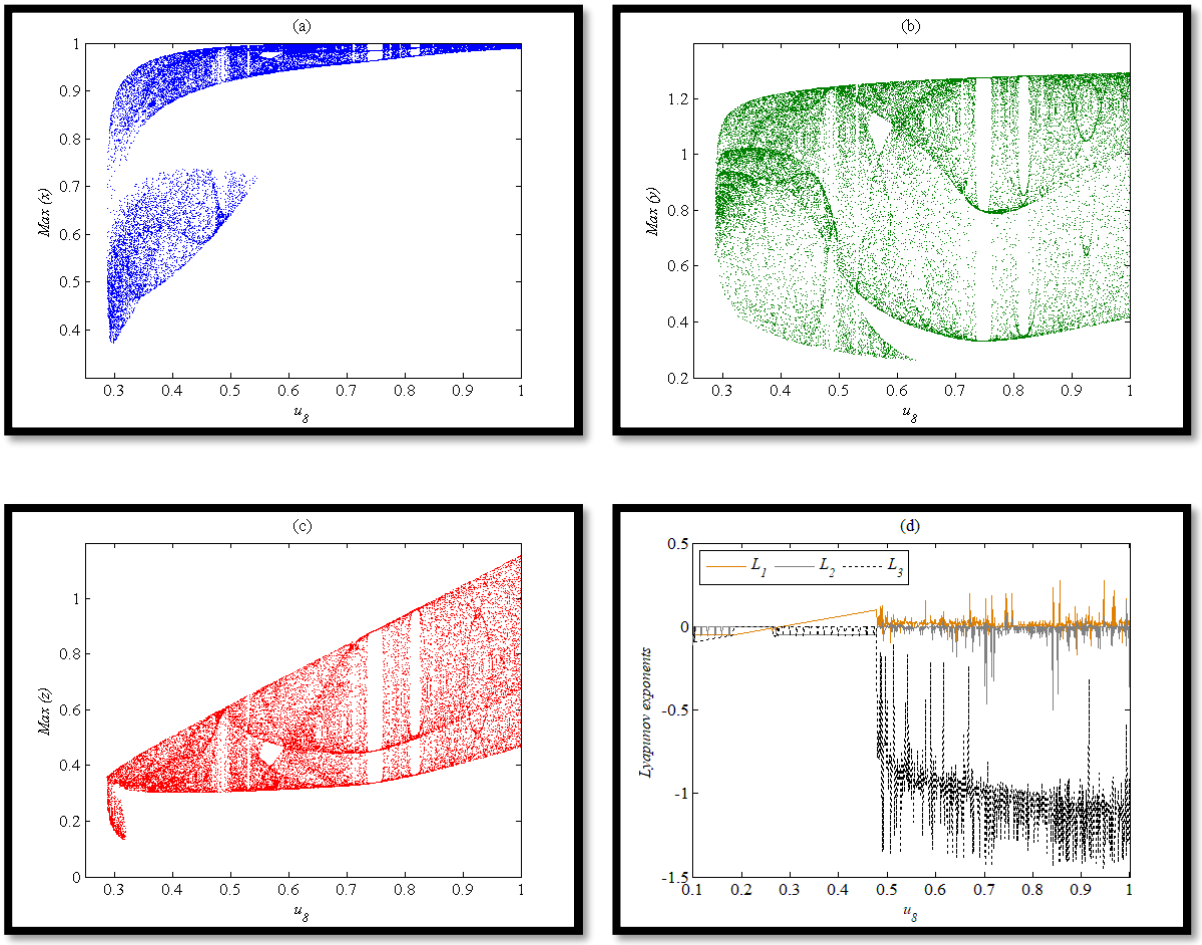

Figure 16. Bifurcation diagrams as a function of u_8. (a) *Max* (*x*) vs. u_8. (b) *Max* (*y*) vs. u_8. (c) *Max* (*z*) vs. u_8. (d) Lyapunov exponents vs. u_8.

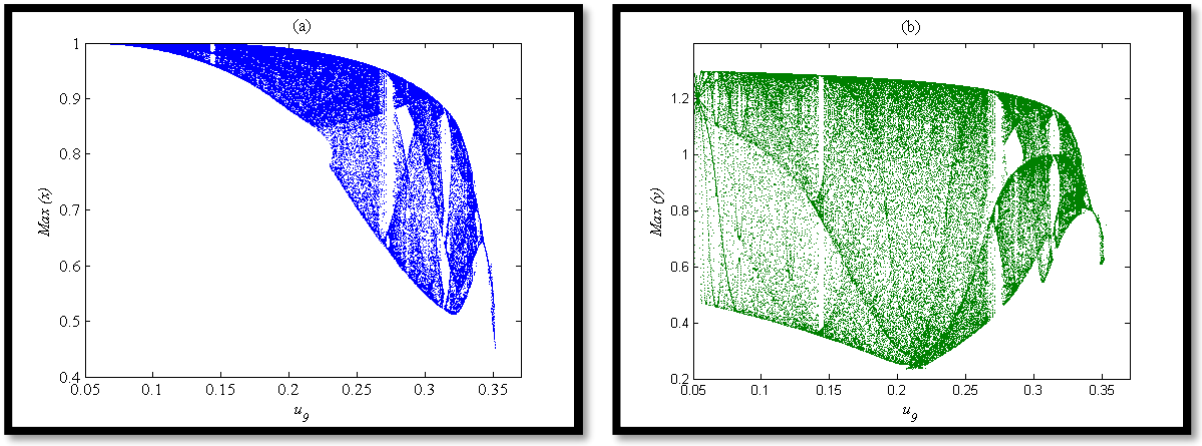

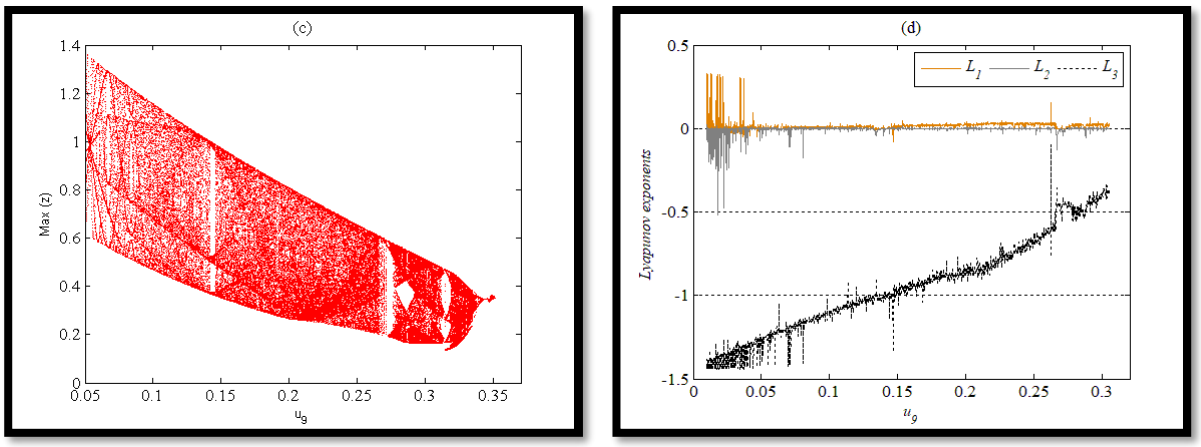

Figure 17. Bifurcation diagrams as a function of u_9. (a) *Max* (x) vs. u_9. (b) *Max* (y) vs. u_9. (c) *Max* (z) vs. u_9. (d) Lyapunov exponents vs. u_9.

According to the above bifurcation diagrams and Lyapunov exponents bifurcation diagrams given in Figures (12)-(17), it is concluded that system (2) has a wide range of complex dynamics including periodic, periodic doubling leading to chaos, and chaos. This range depends on the type of the bifurcation parameter. Furthermore, system (2) is solved numerically. Then the obtained trajectories are plotted in the form of phase portraits and time series for the typical values of parameters, which belong to the bifurcation diagram ranges and outside those ranges. The objective is to explore the set of control parameters on the persistence of the food chain system. All the obtained numerical results are plotted in Figures (18)-(21) and summarized in Table (2).

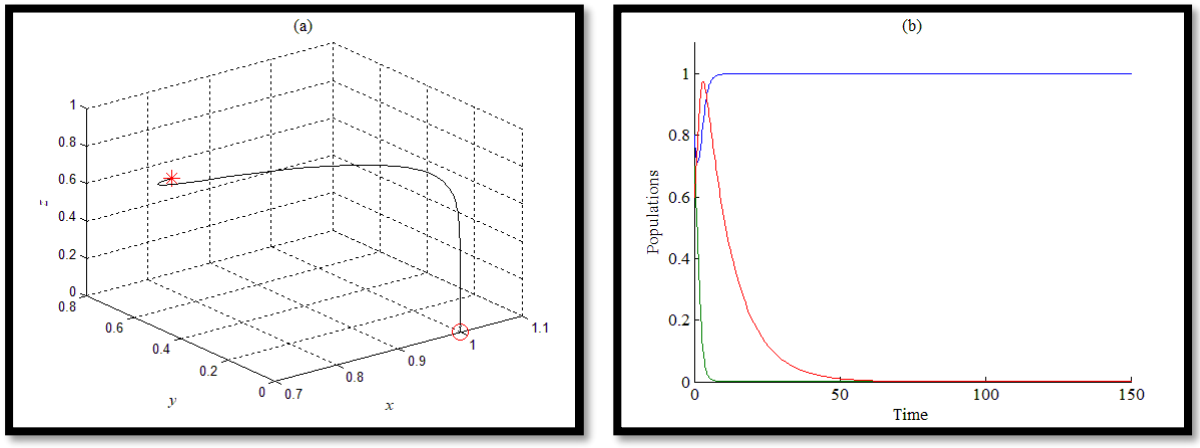

Figure 18. The trajectory of system (2) for the data (8) with $u_4 = 0.3$. (a) Asymptotically stable AEP that given by $(1,0,0)$. (b) Time series of the periodic attractor in (a).

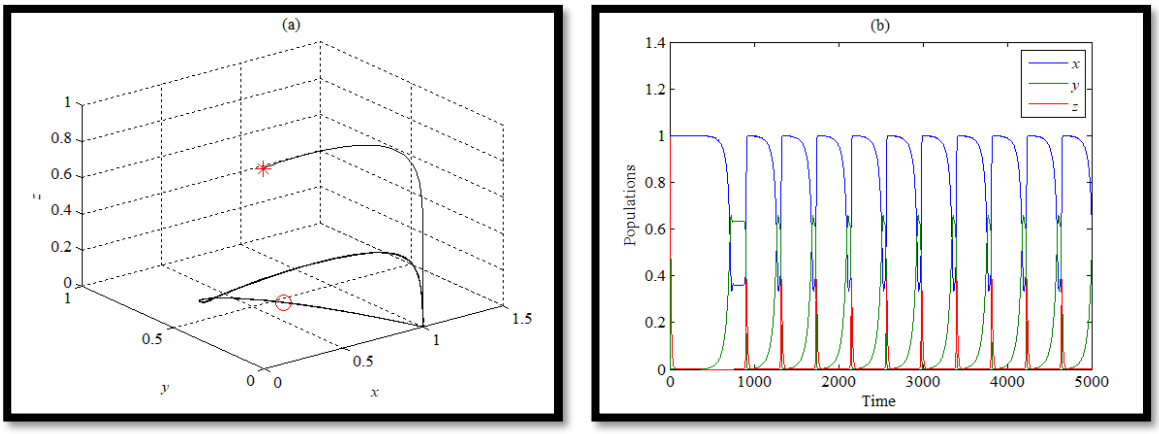

Figure 19. The trajectory of system (2) for the data (8) with $u_4 = 0.35$. (a) 3D periodic attractor. (b) Time series of the periodic attractor in (a).

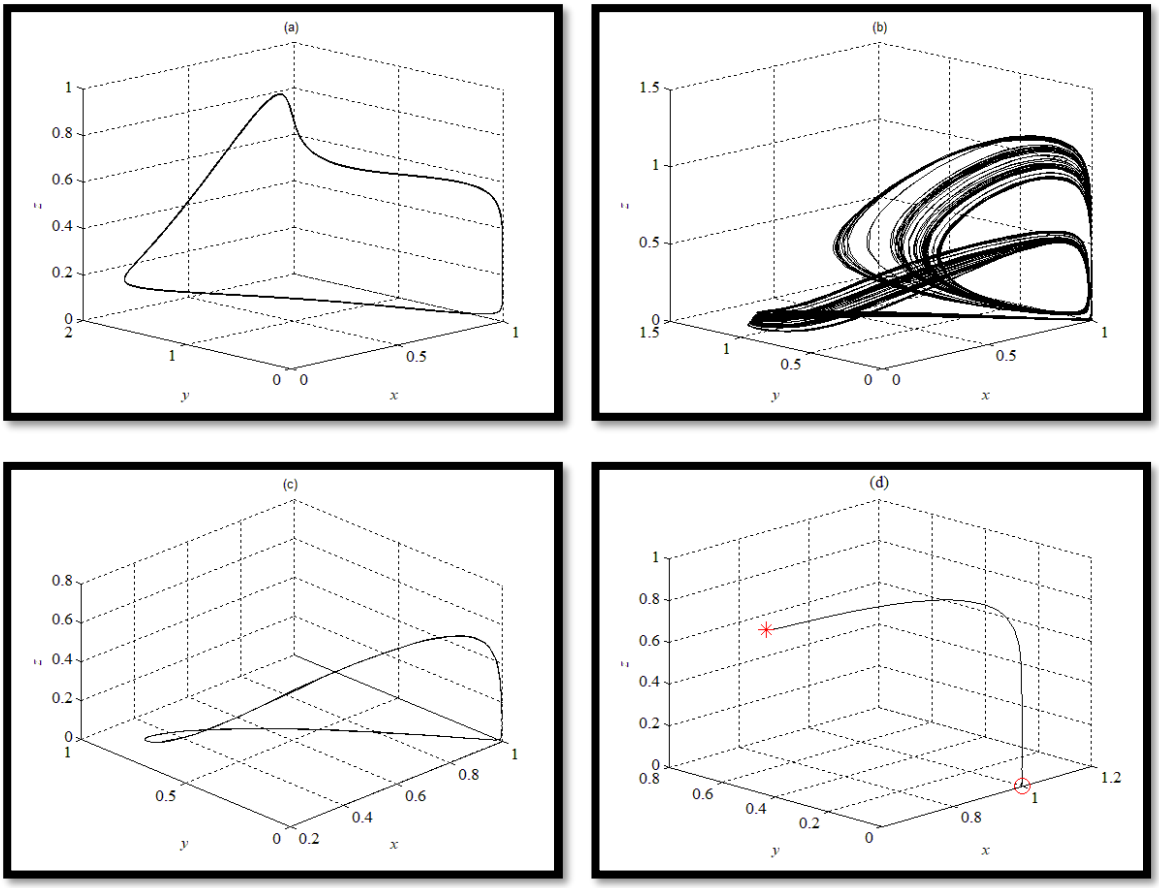

Figure 20. The trajectory of system (2) for the data (8) with different values of u_7. (a) 3D periodic attractor when $u_7 = 0.01$. (b) Strange attractor when $u_7 = 0.15$. (c) 3D periodic attractor when $u_7 = 0.25$. (d) The trajectory approaches to AEP when 3D periodic attractor when $u_7 = 0.45$.

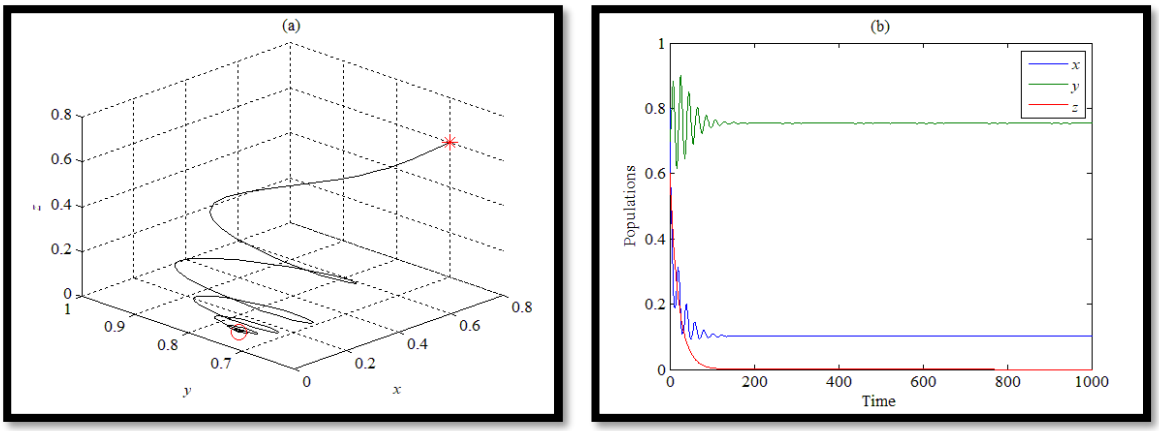

Figure 21. The trajectory of system (2) for the data (8) with $u_9 = 0.4$. (a) Asymptotically stable TPFEP that given by $(0.1,0.75,0)$. (b) Time series of the periodic attractor in (a).

Table 2. The dynamical behavior of the food chain system (2) as a function of parameters using data (8).

The parameter	The range	The dynamical behavior of the system (2)
u_1	$0 \leq u_1 < 1.05$	Chaotic dynamics in between there are windows of periodic
	$1.05 \leq u_1 \leq 4.07$	3D periodic dynamics
	$4.08 \leq u_1 < 37$	Approaches to CEP
	$37 \leq u_1$	Approaches to TPFEP
u_2	$0 < u_2 \leq 0.4$	Chaotic dynamics in between there are windows of periodic
	$0.41 \leq u_2 \leq 0.9$	3D periodic dynamics
	$0.9 < u_2 < 9$	Chaotic dynamics in between there are windows of periodic
	$9 \leq u_2$	Approaches to AEP
u_3	$0 \leq u_3 < 9$	Chaotic dynamics in between there are windows of periodic
	$9 \leq u_3$	3D periodic dynamics
u_4	$0 < u_4 \leq 0.3$	Approaches to AEP
	$0.3 < u_4 \leq 0.55$	3D periodic dynamics
	$0.55 < u_3 \leq 1$	Chaotic dynamics in between there are windows of periodic
u_5	$0 < u_5 \leq 2$	Chaotic dynamics in between there are windows of periodic
u_6	$0 < u_6 \leq 0.6$	3D periodic dynamics
	$0.6 < u_6 \leq 5$	Chaotic dynamics in between there are windows of periodic
u_7	$0 < u_7 \leq 0.03$	3D periodic dynamics
	$0.03 < u_7 < 0.25$	Chaotic dynamics in between there are windows of periodic
	$0.25 \leq u_7 < 0.34$	3D periodic dynamics
	$0.34 \leq u_7 < 1$	Approaches to AEP
u_8	$0 < u_8 \leq 0.28$	Approaches to TPFEP
	$0.28 < u_8 < 1$	Chaotic dynamics in between there are windows of periodic
u_9	$0 < u_9 \leq 0.35$	Chaotic dynamics in between there are windows of periodic
	$0.35 < u_9 < 1$	Approaches to TPFEP

9. DISCUSSION AND CONCLUSION

This study proposes and investigates a three-species Sokol-Howell food chain model. The impact of predation fear on food chain dynamics was investigated. By incorporating the Sokol-Howell kind of functional response that signals such a characteristic, the ability of the anti-predator strategy to defend lower-level species from predation by upper-level species is also incorporated. All of the solution's qualities are discussed. The presence and local stability of all possible equilibrium points are studied. The food chain system's long-term viability is investigated. To examine global dynamics or estimate the basin of attraction of equilibrium sites, the Lyapunov function technique was applied. Local bifurcation conditions near equilibrium points are created. Finally, utilizing various techniques such as bifurcation diagrams, Lyapunov exponent's bifurcation diagrams, and the 3D phase portrait, numerical simulation was widely employed to study the possibility of the existence of complex dynamics.

Throughout the numerical simulation, a hypothetical set of biologically plausible parameter values was used, and the following results were reached. The food chain system (2) is a chaotic system that experiences a variety of attractors, including periodic, long periodic, and chaotic attractors. The fear of predation has a calming influence on the food chain's dynamics. In fact, when the fear rate increased, the chaotic zones shrank and then shifted to periodic, then asymptotically stable CEP. Furthermore, increasing the rate of fear above a certain threshold may lead to predator extinction. Predators become extinct when the anti-predator property in the first level of the food chain system is increased. This does not happen, however, when the second level's anti-predator rate rises and the system shifts from periodic to chaotic. The food chain system will continue to exist as conversion rates rise. Finally, as death rates rise, the food chain system's ability to persist is threatened.

CONFLICT OF INTERESTS

The author(s) declare that there is no conflict of interests.

REFERENCES

[1] F. Hua, K.E. Sieving, R.J. Fletcher, C.A. Wright, Increased perception of predation risk to adults and offspring alters avian reproductive strategy and performance, Behav. Ecol. 25 (2014), 509–519.

[2] D. Duan, B. Niu, J. Wei, Hopf-Hopf bifurcation and chaotic attractors in a delayed diffusive predator-prey model with fear effect, Chaos Solitons Fractals. 123 (2019), 206–216.

[3] K. Kundu, S. Pal, S. Samanta, A. Sen, N. Pal, Impact of fear effect in a discrete-time predator-prey system. Bull. Cal. Math. Soc. 110 (2018), 245–264.

[4] V. Kumar, N. Kumari, Controlling chaos in three species food chain model with fear effect, AIMS Math. 5 (2020), 828–842.

[5] S.K. Sasmal, Population dynamics with multiple Allee effects induced by fear factors – A mathematical study on prey-predator interactions, Appl. Math. Model. 64 (2018), 1–14.

[6] P. Panday, N. Pal, S. Samanta, J. Chattopadhyay, A three species food chain model with fear induced trophic cascade, Int. J. Appl. Comput. Math. 5 (2019), 100.

[7] X. Wang, L. Zanette, X. Zou, Modelling the fear effect in predator–prey interactions, J. Math. Biol. 73 (2016), 1179–1204.

[8] X. Wang, X. Zou, Modeling the fear effect in predator–prey interactions with adaptive avoidance of predators, Bull. Math. Biol. 79 (2017), 1325–1359.

[9] S. Pal, S. Majhi, S. Mandal, N. Pal, Role of fear in a predator–prey model with Beddington–Deangelis functional response, Z. Naturforsch., A. 74 (2019), 581–595.

[10] H. Zhang, Y. Cai, S. Fu, W. Wang, Impact of the fear effect in a prey-predator model incorporating a prey refuge, Appl. Math. Comput. 356 (2019), 328–337.

[11] N.H. Fakhry, R.K. Naji, The dynamics of a square root prey-predator model with fear, Iraqi J. Sci. 61 (2020), 139–146.

[12] K. Sarkar, S. Khajanchi, Impact of fear effect on the growth of prey in a predator-prey interaction model, Ecol. Complex. 42 (2020), 100826.

[13] P. Panday, N. Pal, S. Samanta, J. Chattopadhyay, Stability and bifurcation analysis of a three-species food chain model with fear, Int. J. Bifurcation Chaos. 28 (2018), 1850009.

[14] V. Kumar, N. Kumari, School of Basic Sciences, Indian Institute of Technology Mandi, Mandi, Himachal Pradesh, 175005, India, Controlling chaos in three species food chain model with fear effect, AIMS Math. 5 (2020), 828–842.

[15] H.A. Ibrahim, R.K. Naji, Chaos in Beddington–DeAngelis food chain model with fear, J. Phys.: Conf. Ser. 1591 (2020), 012082.

[16] D. Mukherjee, Impact of predator fear on two competing prey species, Jambura J. Biomath. 2 (2021), 1–12.

[17] A. Abd, R.K. Naji, The impact of alternative resources and fear on the dynamics of the food chain, Int. J. Nonlinear Anal. Appl. 12 (2021), 2207-2234.

[18] F.H. Maghool, R.K. Naji, The dynamics of a Tritrophic Leslie-Gower food-web system with the effect of fear, J. Appl. Math. 2021 (2021), 2112814.